ACS NANO

www.acsnano.org

REVIEW

CRISPR Digital Sensing: From Micronano-Collaborative Chip to Biomolecular Detection

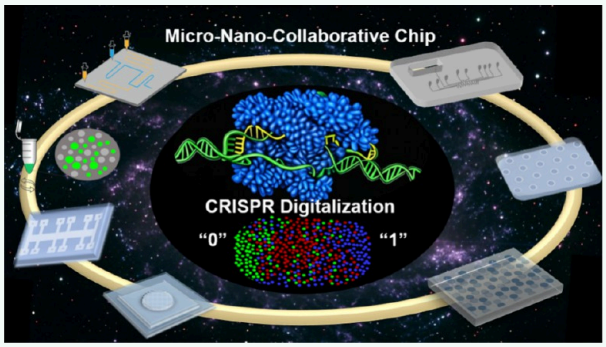
Xinyi Wang,* Longjie Zhong, Wenbin Zhang, Pengde Wu, Minghao Wang,* Dujuan Li,* Linxi Dong, and Gaofeng Wang*

Cite This: https://doi.org/10.1021/acsnano.5c03474

Read Online

ACCESS | Metrics & More | Article Recommendations

ABSTRACT: The Clustered Regularly Interspaced Short Palindromic Repeats (CRISPR) sensing technology proved to be valuable during the COVID-19 pandemic through its sensitivity, specificity, robustness, and versatility. However, issues such as overreliance on amplification, susceptibility to false positives, lack of quantification strategies, and complex operation procedures have hindered its broader application in bioanalysis and clinical diagnostics. The collision between micronano-collaborative chips and CRISPR technology has effectively addressed these bottlenecks, offering innovative solutions for diagnosis and treatment. Unlike conventional micronano chips, micronano digital chips enhance CRISPR's response to trace amounts of target molecules by leveraging highly controllable local environments and compartmentalized microreactors. This advancement improves detection efficiency and revolutionizes traditional *in vitro* bioanalytical processes. First, the working principles, fabrication techniques, and performance metrics of CRISPR-based digital droplet microfluidics and microarray chips are examined. Then, the applications of CRISPR digital sensing chips in bioassays are reviewed, emphasizing their importance in advancing *in vitro* detection systems for gene editing. Finally, the prospects of CRISPR digital sensing technology are explored, particularly its potential for body surface biomonitoring and its broader development opportunities in the biomedical field.



KEYWORDS: *CRISPR digitization, biosensor, micronano chips, droplet microfluidics, microarray chips, biomolecular detection, wearable, multiple detection*

Downloaded via SHANGHAI NORMAL UNIV on May 26, 2025 at 02:20:29 (UTC).
See https://pubs.acs.org/sharingguidelines for options on how to legitimately share published articles.

1. INTRODUCTION

Modern analytical sciences, along with biological and life sciences, strive to attain biological detection that exhibits ultrahigh sensitivity and specificity. In the contemporary context, marked by high population density, extensive mobility, a frenetic pace of life, and severe subhealth issues, the specter of new global diseases looms large. Early precise detection technology can furnish precise details of diseases essential for an immediate medical verdict, effectively curbing mortality rates and improving survival rates. The fight against COVID-19 serves as a prime example, where timely identification and diagnosis were pivotal in mitigating the pandemic's impact.[1] Consequently, propelling the development of precise detection technologies has emerged as a linchpin in safeguarding life and health.

The CRISPR/Cas system is revolutionizing biological detection and bringing more opportunities to achieve this goal.[2] CRISPR technique has been designated as a next-generation gene-editing molecular diagnostic technology,[3] as well as one of the seven technologies[4] of the future by the Journals of Science and Nature. This is an adaptive immune system that widely exists in bacteria and archaea. Bacteria use CRISPR/Cas system as an adaptive defensive mechanism against invading genetic elements.[5] This highly efficient system functions by employing RNA-guided nuclease enzymes to specifically identify and degrade foreign nucleic acids.

According to the arrangement of their loci and distinct proteins, the CRISPR/Cas system is classified into two main classes: Class I and Class II, each with multiple types and subtypes.[6] Class I CRISPR/Cas system, including Types I, III,

Received: February 25, 2025
Revised: May 12, 2025
Accepted: May 13, 2025

© XXXX American Chemical Society

and IV, utilize multisubunit effector complexes.[7] Class II CRISPR/Cas systems rely on a single RNA-guided multidomain Cas protein to recognize and cleave target sequences. Prominent examples in this class are Cas9, Cas12, Cas12f (originally denoted Cas14) of Type V, and Cas13 of Type VI.[8−13] Among these, *in vitro* diagnostic methods based on CRISPR/Cas12, CRISPR/Cas13 and CRISPR/Cas14 are emerging and gaining prominence.[14−18] Once the target DNA is recognized, the RNA-guided CRISPR/Cas12 system cleaves it, generating site-specific double-strand breaks. Then, CRISPR/Cas12 nonspecific cleavage the nearby single-stranded DNA (ssDNA), significantly enhancing DNA detection sensitivity in practical applications.[19] Once the target RNA is recognized, the RNA-guided CRISPR/Cas13 system initiates an effective trans-cleavage activity, which can cleave the surrounding RNA probes nonspecifically, enabling ultrasensitive target RNA recognition.[20] Notably, CRISPR/Cas14 exhibits a distinctive targeting activity against ssDNA without requiring a PAM sequence.[18] This unique property has facilitated their application in nucleic acid detection. CRISPR-based diagnostics have advanced from molecular biology to incorporate multiple COVID-19 assays that have obtained FDA approval.[6,21]

Precision is a prerequisite for the application of detection technologies, RNA-guided Cas proteins in CRISPR/Cas have binding affinities on the picomolar scale for targeted nucleic acids.[22,23] For *in vitro* detection of ultralow abundance analytes (e.g., RNA viruses or miRNAs), Cas proteins must implement strategies to enhance the likelihood of encountering and interacting with the target analyte, thereby producing a signal that is sufficiently elevated above the background in a reasonable amount of time. As a result, CRISPR-based assays are frequently administered in conjunction with numerous amplification techniques.[6] By capitalizing on the excellent specificity and high resolution of CRISPR, numerous scientists have developed one-tube, visualization, and other assays for nucleic acid molecules.[24−28] The CRISPR/Cas13 assay, when used in conjunction with amplification, can result in a one million-fold increase in sensitivity.[29] Feng Zhang groups combined the detection capability of Cas13 with the isothermal amplification to raise the detection limit to the aM level.[30] CRISPR-based amplification-free biosensing methods are not commonly employed. Even though front-end nucleic acid amplification technology has significantly increased the detection sensitivity, the multistep detection process and uncontrollable reaction flow have led to problems with laborious operation, extended detection times, easy cross-contamination, and high false positives, which have become a bottleneck in the practical application of point-of-care testing (POCT).[31,32] On the other hand, in complicated biological samples, pretreatments such as isolation and purification are often required to extract the target. By avoiding these purification steps, CRISPR-based biosensors would be substantially improved, allowing for faster measurement and better handling of the target analyte.

Over the years, a lot of time and effort have been invested by researchers in attempting to overcome these two challenges. No doubt mastering the ability to directly detect biological samples without amplification would extend the practical application of CRISPR technology.[33] Li Wei's group discovered that once activated, the Cas12b mechanism could cut ssDNA at random. They successfully developed the method known as CDetection (Cas12b-mediated DNA detection), which enables the rapid and simple identification of trace DNA.[34] SARS-CoV-2 detection kits based on the CRISPR technology have also been marketed since the COVID-19 pandemic. For instance, the US FDA has authorized the use of CRISPR-based products SHERLOCK[9] and DETECTR[11] in emergency conditions. This is the first time that the FDA has authorized the use of CRISPR technology for the identification of infectious disease identification. Even though the relevant technology has already reached a stage of intense competition, the aforementioned two components of the problem remain unresolved, limiting the technology's potential for further clinical transformation and application.

CRISPR digital sensing provides a viable platform for future CRISPR-based diagnostic applications.[35−41] Based on droplet microfluidic chips and microarray chips, samples can be exquisitely confined within the picoliter to nanoliter scale range. This precise confinement, a consequence of the confinement effect, leads to a substantial increase in the relative concentration of targets. As a direct result, the sensitivity of the detection system is markedly enhanced. Direct quantification of target biomolecules becomes feasible by measuring the fluorescence end point counts in each partition. This approach obviates the necessity for endogenous references, enabling absolute quantification of biomolecules. Moreover, it allows for single-nucleotide-specific detection, which is crucial for high-resolution molecular analysis.[42,43] Compared with conventional CRISPR sensing, digital CRISPR sensing is more robust for absolute measurement. It can effectively amplify single molecules and exhibit greater resistance to reaction inhibitors, ensuring more reliable and accurate results. With the rapid advancement of micronano processing technology, two distinct types of CRISPR-based digital sensing chips have emerged: droplet microfluidic and microarray.

Research in magnetic separation has enabled the integration of nucleic acid extraction, purification, amplification, and detection into a single digital biochip. Magnetic bead-modified probes can capture targets in complex samples through specific chemical reactions. By application of an external magnetic field, these magnetic beads can be rapidly and efficiently captured and separated from the reaction system. Additionally, the magnetic field facilitates the removal of nonspecifically adsorbed substances, ensuring high detection accuracy and specificity.[44−46] Wu et al. designed a droplet magnetic-controlled microfluidic chip that integrates nucleic acid extraction, amplification, and detection.[47] This chip leverages the interfacial tension between droplets and the oil phase, while permanent magnets automate the movement, splitting, and fusion of droplets to maintain a closed environment. This design prevents cross-contamination and aerosol formation, enabling direct in situ amplification. Magnetic-controlled microarray chips have been successfully validated for highly sensitive and specific biomolecule detection, capable of capturing single molecules and detecting fluorescence signals. Currently, a variety of fabrication methods exist for microarray chips, which allow for the simultaneous analysis of multiple targets.[48,49]

This review provides a comprehensive overview of the latest advancements in CRISPR digitization, covering both amplification and amplification-free strategies (Figure 1). It emphasizes the integration of micronano collaborative chips—such as droplet microfluidic chips and microarray

https://doi.org/10.1021/acsnano.5c03474
ACS Nano XXXX, XXX, XXX−XXX

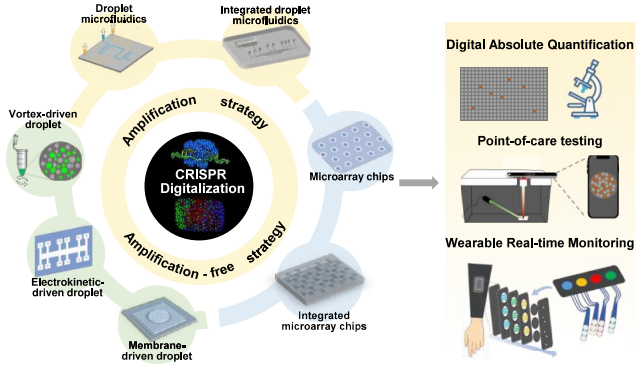


Figure 1. Applications of CRISPR digital biosensors based on micronano collaborative chips.

chips, with CRISPR sensing technologies to address key challenges in biodetection and to advance digital concepts for diagnosis and therapy. It systematically summarizes and compares the performance metrics of various CRISPR digital platforms including sensitivity, specificity, and throughput. Rather than focusing solely on qualitative research, this review emphasizes digital absolute quantification, POCT, and wearable real-time monitoring using CRISPR digital biosensors. These technologies enable biomolecular detection in real-world samples with minimal user intervention, providing automated testing to reduce false positives and streamline pretreatment processes. The potential of CRISPR digital sensing technology is explored, particularly its high accuracy in identifying single-base mutations, its multiplexing capabilities, and its potential for integrating diagnosis and therapy. Finally, the review concludes with a comprehensive outlook and prospective discussion of this rapidly evolving field.

2. PRINCIPLE OF CRISPR-BASED MICRONANO DIGITAL SENSING CHIPS

Table 1 provides an overview of the features and capabilities of CRISPR-based digitization chips, including droplet microfluidics biochips, microarray biochips, and other unique digital CRISPR biochips for single- or multiple- target detection. CRISPR-integrated digital sensing chips have distinct advantages over those combined with other nucleic acid detection methods. CRISPR's unique nucleic acid recognition mechanism provides ultrahigh specificity, enabling precise discrimination of highly similar sequences. In terms of sensitivity, CRISPR-integrated digital sensing chips can achieve single-molecule detection, outperforming some traditional techniques. They are more user-friendly with an integrated design that effectively reduces errors and contamination risks. Additionally, their programmable nature enables a powerful multiplex-detection function, allowing for the simultaneous detection of multiple targets on one chip. Thus, this technology is widely applied in emerging fields such as liquid biopsy and viral mutation monitoring.

The volume of droplets in droplet-based microfluidics biochips is consistently at the picoliter level, while the chamber volume in microarray biochips is consistently at the nanoliter level. Generally, the volume of the sensing unit is associated with the detection limit. The volume of the droplets could be regulated by the oil-to-aqueous phase flow rate ratio and the size of the microfluidic channel. The lower volume of the microarray chamber needs more precise micronano processing technology. Both of the chips have amplification and amplification-free strategies for biomolecular detection. For amplification strategies, the uniquely shaped chips are utilized to prevent cross-contamination caused by amplification reagents. For amplification-free strategies, the special CRISPR assay design, precise dimensions, and fine machining of droplets or microchambers are required to lower the detection limit. With the development of CRISPR and micronano technologies, the limit of detection (LOD) of amplification-free CRISPR digital biosensors could be lower as well as amplification strategies. The detailed design of the micronano collaborative chip applied for CRISPR digitization is discussed in this section.

2.1. Droplet Microfluidic Sensing Chips. *2.1.1. Flow-Based Microfluidic Biochips.* Utilizing micronanotechnology, the flow-based microfluidic biochips which is based on the fluid focusing principle, shears the oil and aqueous phases to achieve CRISPR digital sensing detection.[65−69] This process quickly and precisely divides the sample fluid into multiple independent microdroplets in the picoliter (pL) to nanoliter (nL) range.[70−74] Microdroplets enhance local molecule concentration based on the confinement effect, enabling ultrasensitive marker detection and response sensitivity.[75−78] Additionally, it enables rapid and controlled fluid mixing in the droplet reactor, thereby reducing reaction times. Achieving digital quantitative marker detection can be done by counting the percentage of positive droplets. The droplet volume may be controlled by the micronanofabrication processing and the oil-to-aqueous phase flow rate ratio. Thus, droplet microfluidic sensing chips are promising to offer low cost, tiny volume, scalable size, and high throughput for multiple-step parallel operations.

As shown in Figure 2, various micronano droplet microfluidic structures have been developed to advance CRISPR digital sensing technology. To address the issue of false positives in CRISPR assays, several innovative designs have been implemented. These include a microinjector serving as a postinjection device (Figure 2a),[56] a Y-channel structure that separates the target from the amplification reagent (Figure 2b),[50] and a two-step microfluidic structure that integrates amplification and detection processes (Figure 2c).[51] By physically isolating the target and amplification reagent, premature amplification is prevented, ensuring that the amplification reaction is initiated only after droplet formation. To enhance the control of the CRISPR sensing process, a microfluidic chip utilizing negative pressure actuation was developed (Figure 2d).[57] Additionally, to simplify fabrication requirements, membrane-based (Figure 2e)[54] and vortex-based technologies (Figure 2f)[58] were ingeniously designed for rapid and efficient droplet generation, eliminating the reliance on shear forces between the oil and aqueous phases. Furthermore, multiplexed droplet microfluidic devices have been engineered to enable simultaneous multitarget detection (Figure 2g),[59] significantly expanding the versatility and applicability of CRISPR-based sensing platforms.

2.1.2. Digital Microfluidic Biochips. The working principle of digital microfluidic biochips (DMFB) is mainly based on electrowetting. It enables precise manipulation of discrete picoliter (pL) to microliter (μL) droplets through an electrode array, facilitating various biological and chemical analyses.[79] The most widely used droplet actuation mechanism in DMF chips is electrowetting on dielectric (EWOD). The chip consists of a bottom plate with an electrode array and a top

https://doi.org/10.1021/acsnano.5c03474
ACS Nano XXXX, XXX, XXX−XXX

Table 1. Summary of Digital CRISPR Biosensors Based on the Micronano Collaborative Chip[a]

Partitioning	Name	Target	Method	Digital platform	Volume	LOD	Conditions	ref.
Flow-Based Microfluidic Biochips	PADLOCK-CRISPR	HPV 16	One-pot RPA-CRISPR/Cas13a	Postinjection microfluidic device	~41 pL	10 copies/μL	30 min; 37 °C	50
	DropCRISPR	*Salmonella typhimurium strain*; plasmid	LAMP-CRISPR/Cas12a	Two-step microfluidic system with a picoinjector	~14 pL	10^2CFU/mL; 3 fM	50 min 63 °C, 10 min 42 °C 50 min; 63°C, 10 min; 42 °C	51
	ddRECD	SARS-CoV-2	RT-LAMP-CRISPR/Cas12b	T-junction microfluidic device	~0.3 nL	14 copies/μL	120 min; 60 °C	52
	ddHECTelo	Telomerase activity	Hyperbranched amplification enhanced CRISPR/Cas12a	Vortex-LongGene Real-Time PCR instrument	/	0.6 cells/μL	80 min; 42 °C	53
	STAMP-CRISPR	HIV-1	Amplification-free STAMP-CRISPR/Cas13a	Commercially polycarbonate track etch membrane	13 pL	1 fM	30 min; 37 °C	54
	Ultralocalized Cas12a	ASFV	Amplification-free CRISPR/Cas12a	T-junction microfluidic droplet chip	~pL	17.5 copies/μL	60 min; 37 °C	55
	CRISPR/Cas12a-crRNA duplexes	EBV DNA	Double crRNA-mediated cis-cleavage	QX200 Droplet Digital PCR system (Bio-Rad, USA)	/	5 copies/μL	60 min; 45 °C	41
	MEDICA	HPV 16 HPV 18	One pot RPA-CRISPR/Cas13a	Y-shaped microfluidic chip	~pL	1.1 copies/μL	25 min; 37 °C	56
	Ultralocalized Cas13a	miRNAs; 16S rRNAs; SARS-CoV-2	Amplification-free CRISPR/Cas13a	T-junction microfluidic droplet chip	~pL	100 aM; 6 copies/μL; 6 copies/μL	60 min; 37 °C	57
	PddCas	HPV 18; SARS-CoV-2	Amplification-free CRISPR/Cas12a, CRISPR/Cas13a	Vortex mixer spinning	10−100 μm (D)	100 aM; 10 aM	20 min; 40 °C	58
	M-D3	HPV 16 HPV 18	RPA-CRISPR/Cas12a	Dual-droplet microfluidic chip combining pressure/vacuum	34 μm (D)	1 aM	30 min; 39 °C	59
Digital Microfluidic Biochips	DFM-Cas12a	*S. aureus*	RPA-CRISPR/Cas12a	Electrowetting on dielectric based microfluidic chip	μL	32 CFU/mL	55 min; 95 °C, 37 °C	40
Microarray Biochips	dWS-CRISPR	SARS-CoV-2	One-pot RT-DAMP-CRISPR/Cas12a	QuantStudio 3D digital chip	~0.7 nL	5 copies/μL	90 min; 50 °C	60
	deCOViD	SARS-CoV-2	One-pot RPA-CRISPR/Cas12a	QuantStudio 3D Digital PCR 20K Chip	~0.7 nL	1 GE/μL	30 min; 42 °C	37
	RADICA	SARS CoV-2	One pot RPA-CRISPR/Cas12a	Clarity digital chip	~1.336 nL	~0.897 copies/μL	60 min; 42 °C	36
	WS-RADICA	SARS-CoV-2	One-pot RT-LAMP-CRISPR/Cas12b	Clarity digital chip; QIAcuity digital nanoplate.	~1.336 nL; ~0.91 nL	1 copies/μL	60 min; 60 °C	61
	Adsorption-free 3D assay	*Salmonella*	One-pot RPA-CRISPR/Cas12 with dual-crRNA	A self-priming liquid-dispensing digital microarray chip	~100 μm (D)	0.2 cells/mL	30 min; 39 °C	62
	CASMART	EGFR L858R	One-pot RPA-CRISPR/Cas12a	Commercially QuantStudio 3D digital chip	~0.7 nL	0.3 copies/μL	60 min; 42 °C	63
	dCRISPR	SARS-CoV-2	Magnetic beads integrated CRISPR/Cas13a	High-integrated microwell array	~fL	2 aM	50 min; 32 °C	38
	SATORI	SARS-CoV-2	Amplification-free CRISPR/Cas13a	Microarray device	~3 fL	~5 fM	5 min; 37 °C	64

[a]PADLOCK: Picoinjection Aided Digital reaction unLOCKing; DropCRISPR: digital droplet-based platform; DMF: digital microfluidic chip; STAMP: self-digitization through Automated Membrane-based Partitioning; ddRECD: droplet digital reverse transcription loop-mediated isothermal amplification (RT-LAMP) enhanced Cas12b-based RNA detection; ddHECTelo: droplet digital hyperbranched amplification enhanced CRISPR/Cas12a-based telomerase detection platform; MEDICA: Microfluidics-Enabled Digital Isothermal Cas13a Assay; PddCas: polydisperse droplet digital CRISPR/Cas-based assay; M-D3: microfluidic dual-droplet device; dWS-CRISPR: digital warm-start CRISPR; deCOViD: digitization-enhanced CRISPR/Cas-assisted one-pot virus detection; RADICA: RApid DIgital CRISPR Approach; WS-RADICA: Warm-Start RApid DIgital CRISPR Approach; SATORI: CRISPR-based amplification-free digital RNA detection; 3D assay: direct digital dual-crRNAs assay; CASMART: CRISPR Assoaciated Mutation Allele Rapid Test; dCRISPR: Digital CRISPR; ASFV: African swine fever virus.

https://doi.org/10.1021/acsnano.5c03474
ACS Nano XXXX, XXX, XXX−XXX

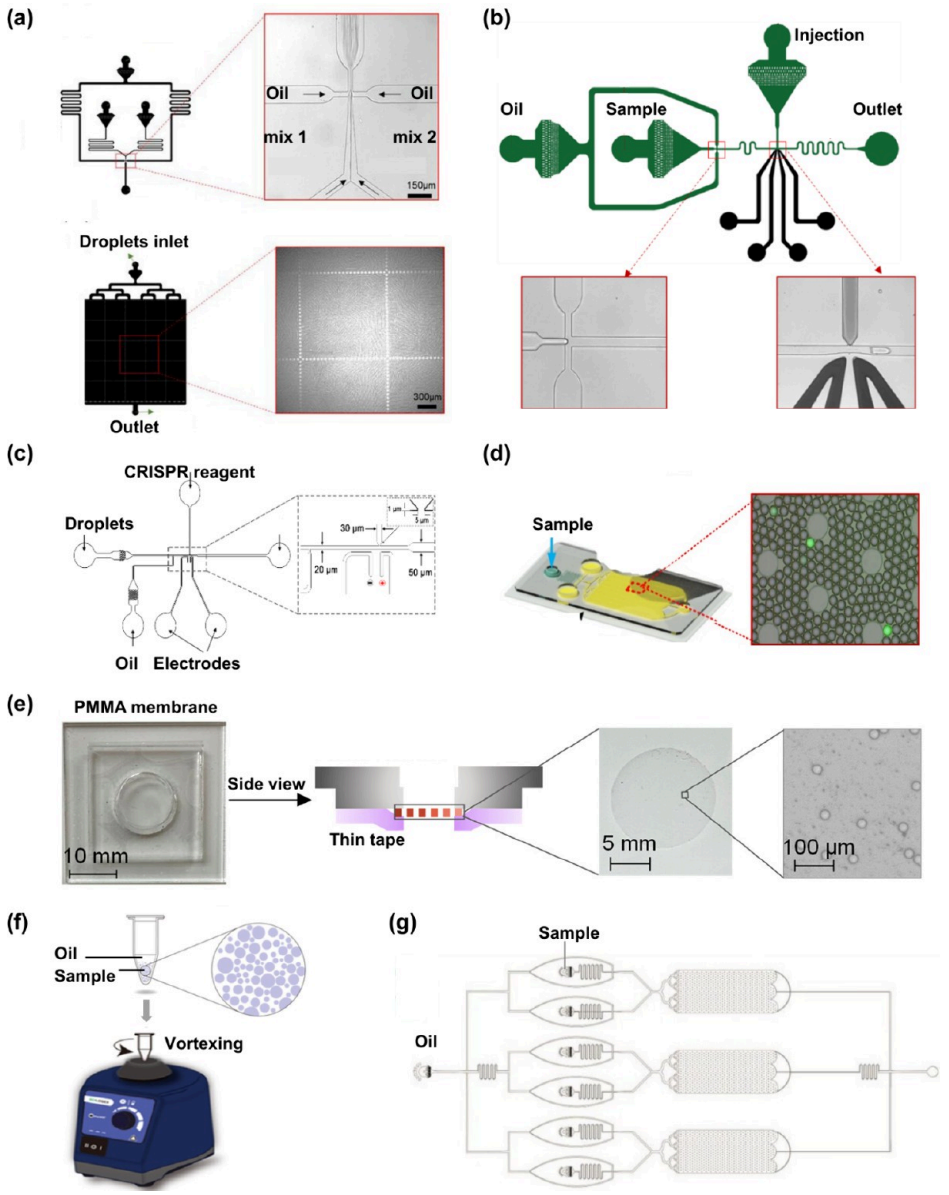


Figure 2. Structure of CRISPR-enabled flow-based microfluidic biochips. (a) Micronano structure with Y-shaped channel inlet. Adapted with permission from ref 56. Copyright 2022, American Chemical Society. (b) A microinjector-based postinjection micronano structure. Adapted with permission from ref 50. Copyright 2022, Elsevier. (c) A microinjector-based, two-step microfluidic structure. Adapted with permission from ref 51. Copyright 2022, Elsevier. (d) A negative pressure actuation micronano structure with syringe pumping. Adapted with permission from ref 57. Copyright 2021, American Chemical Society. (e) Structure with PMMA membrane-assisted droplet generation strategy. Adapted with permission from ref 54. Copyright 2023, American Chemical Society. (f) Structure with vortex-assisted droplet generation strategy. Adapted with permission from ref 58. Copyright 2023, American Chemical Society. (g) Multiplexed micronano structure of multiple detections. Adapted with permission from ref 59. Copyright 2023, American Chemical Society.

plate. The bottom electrode plate is patterned through processes such as photolithography and etching and is coated with a dielectric layer and a hydrophobic layer. The top plate, usually made of glass or plastic, is also coated with a hydrophobic layer. When a continuous potential is applied to the electrode array through a computer-controlled program, the interfacial tension between the droplet and the electrode surface changes, enabling actuation of the droplet. This actuation method allows droplets to be moved, merged, split, and dispensed on the chip surface. It is like building a miniature "liquid manipulation factory" on the chip, which can precisely control the behavior of each droplet.

As shown in Figure 3, the digital microfluidic biochip consists of two parallel glass plates, including a bottom electrode plate and a top indium−tin oxide (ITO) glass. The bottom electrode plate forms an electrode array through photolithography and wet etching. Subsequently, a 15-μm-high layer of SU-8 photoresist is coated as a dielectric layer. The surface of the chip is hydrophobically treated, and combined with the coverage of fluorocarbon oil, it can effectively reduce nucleic acid adsorption and contamination, minimize external interference, and, at the same time, reduce droplet evaporation. The chip is equipped with multiple reservoirs for storing various reagents required for the reaction, such as lysis buffer, RPA mixture, Cas12a mixture, etc., providing a material basis

https://doi.org/10.1021/acsnano.5c03474
ACS Nano XXXX, XXX, XXX−XXX

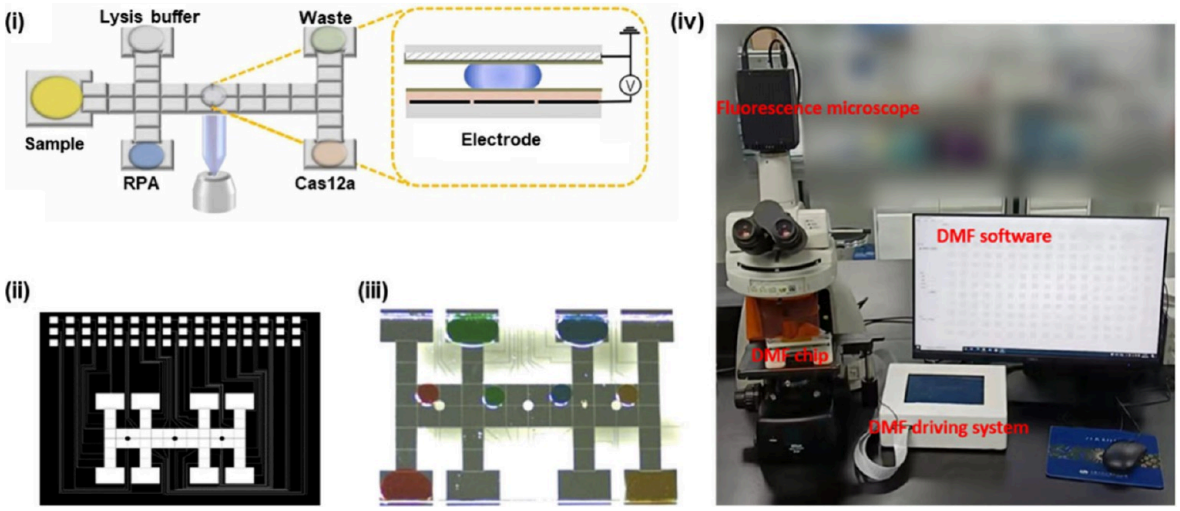


Figure 3. Structure of CRISPR-enabled digital microfluidic biochips. Adapted with permission from ref 40. Copyright 2023, Elsevier. (i) Micronano structure where droplets are driven by the electrowetting on dielectric technique. (ii) CAD design of bottom plate of DMF-Cas12a biochip. (iii) Photograph showing the four droplets successively generated from different reservoirs with good uniformity and quality. (iv) Automated device of DMF-Cas12a method, containing the DMF chip, microfluidic software, DMF driving system (function generator), and fluorescence microscope.

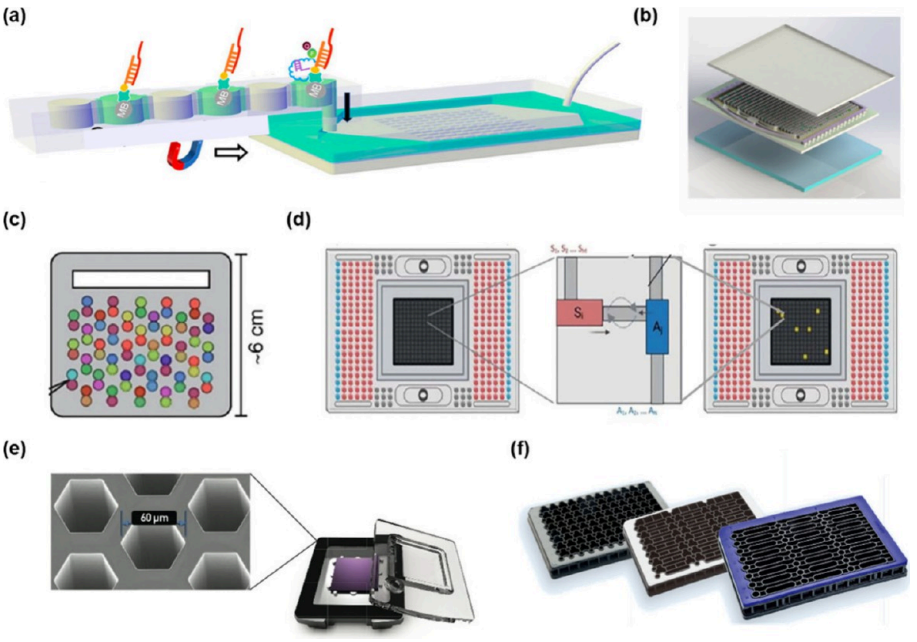


Figure 4. Structure of CRISPR-based micronano digital microarray chips. (a) Micronano structure with highly integrated pretreatment and detection module. Adapted with permission from ref 38. Copyright 2023, American Chemical Society. (b) A self-priming liquid-dispensing digital microarray chip. Adapted with permission from ref 82. Copyright 2021, Elsevier. (c) A microarray chip with multiplexing. Reprinted with permission under a Creative Commons CC-BY 4.0 License from ref 80. Copyright 2020, Springer Nature. (d) Multiplexed microarray chip combined with commercial Fluidigm chips and equipment. Reprinted with permission under a Creative Commons CC-BY 4.0 License from ref 81. Copyright 2022, Springer Nature. (e) Commercial QuantStudio 3D digital microarray chip. (f) Commercial QIAcuity digital microarray nanoplate.

for subsequent reactions. It was shown that the coefficients of variation of droplet volumes dispensed from the same reservoir or different reservoirs were small, 3.3% and 4.8%, respectively, which demonstrated the good homogeneity and stability of droplet generation on the DMFB and ensured the reliability of the reaction.

2.2. Microarray Sensing Chips. Millions of nanoliter or femtoliter micropores, carved by micronano manufacturing processes, make up the microarray chip. Accurate quantitative results are produced by accurately controlling the reaction volume and distributing the sample uniformly throughout the equal volume of microporous chambers.[6,38,80,81] It solves the shortcomings of the droplet microfluidic chip, which makes it difficult to control the droplets and ensure a precise uniform droplet size.

As shown in Figure 4, several micronano microarray sensing chips were developed to facilitate the development of CRISPR digital sensing. Based on advances in micronano fabrication

https://doi.org/10.1021/acsnano.5c03474
ACS Nano XXXX, XXX, XXX−XXX

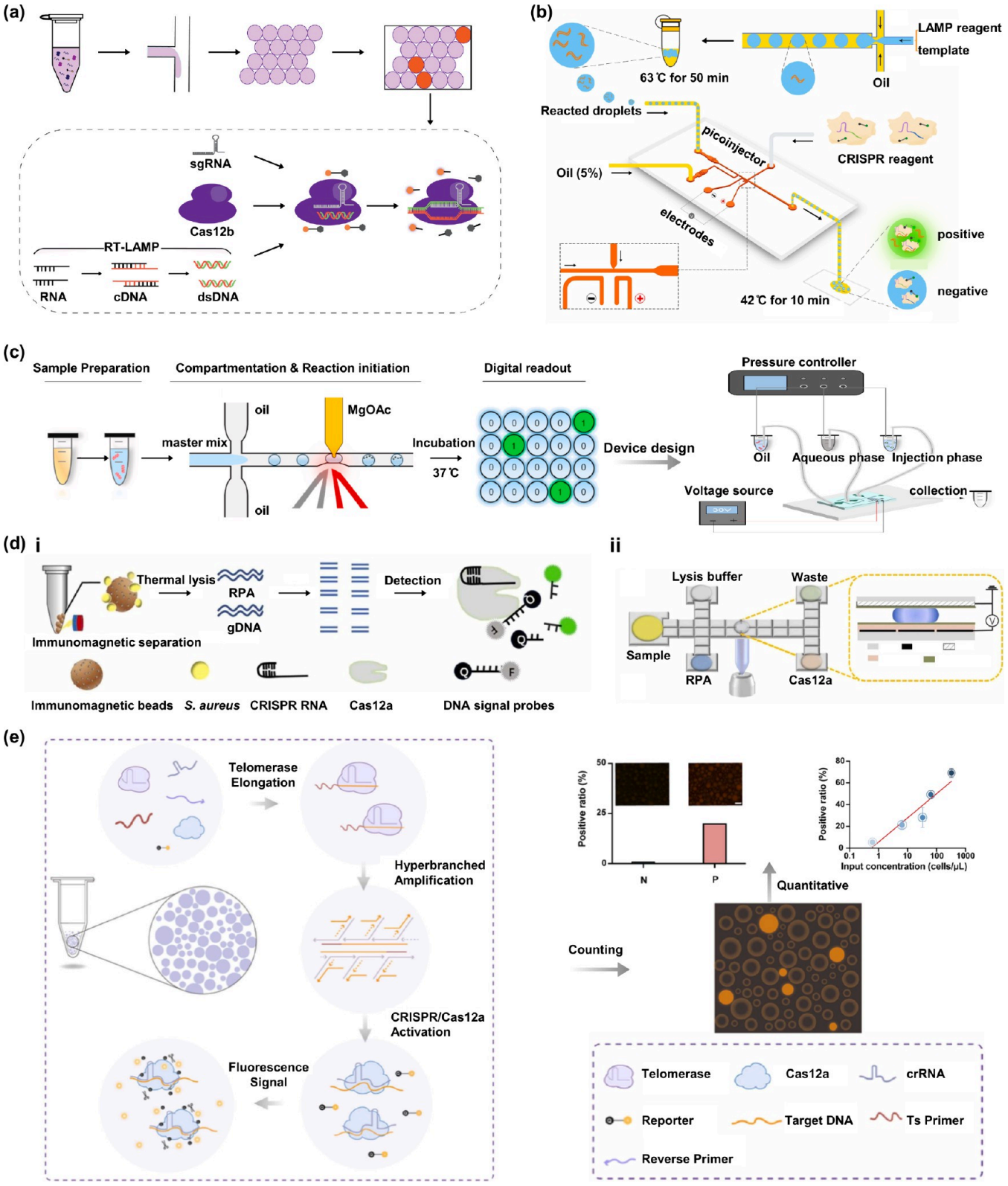


Figure 5. CRISPR-based amplification digital sensing with a droplet microfluidic chip. (a) Schematic diagram of ddRECD biosensor based on RT-LAMP-CRISPR/Cas12b and T-junction droplet microfluidic chip. Adapted with permission from ref 52. Copyright 2021, Elsevier. (b) Schematic diagram of DropCRISPR biosensor based on LAMP-CRISPR/Cas12a and two-step droplet microfluidic system with a picoinjector. Adapted with permission from ref 51. Copyright 2022, Elsevier. (c) Schematic diagram of PADLOCK-CRISPR biosensor based on postinjection microfluidic device and one-pot RPA-CRISPR/Cas13a. Adapted with permission from ref 50. Copyright 2022, Elsevier. (d) Schematic diagram of DMF-Cas12a biosensor. Adapted with permission from ref 40. Copyright 2023, Elsevier. i: Immunomagnetic beads-based samples pretreatment; ii: Detection process based on electrowetting on a dielectric. (e) Schematic diagram of the ddHECTelo biosensor based on vortex-assisted droplet generation for assisted telomerase activity detection. Adapted with permission from ref 53. Copyright 2023, Elsevier.

https://doi.org/10.1021/acsnano.5c03474
ACS Nano XXXX, XXX, XXX−XXX

technology, the process units required for target detection, including sample pretreatment, nucleic acid extraction, target sequence amplification, and signal detection, can be partly or entirely integrated into a single microarray chip (Figure 4a).[38] This helps to automate and integrate detection, improve detection efficiency, minimize operational errors, lower detection costs, and reduce the risk of aerosol contamination. To eliminate the external power supply and reduce the sample loading time, a self-priming liquid-dispensing digital microarray chip was designed (Figure 4b).[82] Multiplexed microarray chips are designed to achieve multigene detection (Figure 4c, d).[80,81] Commercially available microarray chips are being produced to support the development of automated droplet screening assays and miniature analytical tools (Figure 4e, f).

Both droplet microfluidic chips and microarray chips have great potential in CRISPR digitization, with their own characteristics and application scenarios. Micronano collaborative chips have greatly facilitated the application of CRISPR digital sensing and promoted their development in healthcare and related industries. The ease of mass production and lower manufacturing costs of CRISPR digital sensing chips facilitate their popularization and dissemination.

3. DIGITAL CRISPR BIOSENSORS BASED ON DROPLET MICROFLUIDIC CHIPS

The integration of CRISPR with droplet microfluidic chips has advanced digital CRISPR biosensors, balancing sensitivity and accuracy.[83−85] This section highlights progress in amplification-based and nonamplification-based digital CRISPR biosensors, showcasing improved performance and practicality. It also outlines steps for future precise detection technologies and explores applications in biological detection.

3.1. Amplification Strategy. Leveraging CRISPR technology, platforms such as DETECTR,[11] SHERLOCK,[9] HOLMES,[86] and HOLMESv2[87] have been developed, offering high-sensitivity and high-specificity nucleic acid detection. To achieve ultrasensitive detection for clinical diagnostics, isothermal amplification approaches, like loop-mediated isothermal amplification (LAMP)[88] and recombinase polymerase amplification (RPA)[89] have been integrated into CRISPR-based droplet microfluidic chips. Compared with conventional qPCR, isothermal amplification techniques are more resource-friendly. They amplify nucleic acids isothermally, removing the need for thermal cyclers. This cuts down on equipment costs and reduces the requirements for specialized skills and laboratory facilities, expanding their application scope.

Luo et al. integrated the CRISPR/Cas12b system and RT-LAMP technology to develop the ddRECD platform (Figure 5a).[52] A simple T-junction droplet microfluidic chip was utilized to generate ∼0.3 nL of droplets for digital viral RNA detection. On this platform, Cas12b binds to sgRNA, forming a complex. Once the complex identifies the target DNA amplified by RT-LAMP, it triggers the nonspecific trans-cleavage activity of Cas12b, cutting a single-stranded DNA reporter. This cleavage separates the fluorescent and quenching groups, producing a fluorescent signal for quantification. The ddRECD platform has an LOD of 14 copies/μL and can accurately distinguish samples with very small concentration differences. While traditional RT-LAMP often produces false positives, Cas12b's sequence-specific binding helps reduce false signals caused by primer dimers or spurious amplicons. Tests comparing RT-LAMP and ddRECD on negative samples showed that ddRECD effectively eliminates false positives, significantly improving the detection specificity.

Similarly, Wu et al. combined LAMP and CRISPR/Cas12a to establish the DropCRISPR platform (Figure 5b).[51] They optimized the CRISPR/Cas12a system using a dual-gRNA strategy, where each target recruits two Cas12a proteins, enhancing trans-cleavage activity and amplifying the signal. The platform features a unique two-step microfluidic design consisting of a droplet generator and a picoinjector. First, the droplet generator produces stable droplets containing LAMP reagents for isothermal amplification. As the amplified droplets flow through the chip, an electric field weakens the water−oil interface, allowing the picoinjector to inject CRISPR/Cas12a reagents. This design resolves compatibility and interference issues caused by the different optimal temperatures required for LAMP and CRISPR/Cas12a, ensuring efficient reactions. The DropCRISPR platform achieves a detection limit of 3 fM for the invA-containing model plasmid and 10^2 CFU/mL for *Salmonella typhimurium* (St). It is 100 times more sensitive than traditional bulk LAMP and 10 times more sensitive than bulk LAMP/Cas12a reactions. The two-step microfluidic system effectively addresses temperature-related compatibility issues, improving the detection accuracy. Additionally, the platform can detect *Salmonella* in raw samples like LB medium and milk without requiring nucleic acid extraction. Compared with the ddRECD platform, DropCRISPR, despite its advantage in temperature compatibility, shows limited improvement in detection sensitivity. This may be due to the separation of amplification and detection into two stages, which complicate process integration and introduce errors in quantifying initial target concentrations.

RPA, with a reaction temperature near ambient (37−42 °C), is well-suited for developing one-pot CRISPR digital systems.[90,91] Unlike PCR or LAMP, it starts without a hot start. Adding magnesium acetate (MgOAc) initiated the reaction, even at room temperature. Nevertheless, premature bulk amplification during prediscretization sample analysis often overestimates the target concentration, so quantitative accuracy remains a challenge for the RPA-CRISPR system.

Cui et al. combined RPA-CRISPR/Cas13a with a post-injection microfluidic chip to develop the PADLOCK platform (Figure 5c).[50] The picoinjector features a pressurized injection channel and a pair of electrodes. This unique design generates a Laplace pressure barrier between the injection phase and the oil phase. The nozzle's small diameter ensures sufficient Laplace pressure for stable and consistent reagent injection. Leveraging the Venturi effect, which decreases fluid pressure when the fluid flows through a constricted section of the tube, enhances the contact between the droplet and the injection phase. First, a MgOAc-deprived RPA master mix was partitioned into droplets. Then, MgOAc was injected into the droplets via the picoinjector to initiate the reaction, avoiding premature amplification. Droplets containing target nucleic acids initiate amplification reactions and emit fluorescence, marking them as positive droplets ("1"). Droplets without targets remain dark, marking them as negative droplets ("0"). Using a fluorescence microscope and ImageJ software, the platform counts the proportion of positive droplets and applies a Poisson distribution to achieve single-molecule detection with a limit of detection (LOD) of 10 copies/μL and a high signal-to-noise ratio (S/N ratio >6). When tested on 22 clinical samples for HPV16 viral load detection, the PADLOCK platform showed 100% agreement with qPCR

https://doi.org/10.1021/acsnano.5c03474
ACS Nano XXXX, XXX, XXX−XXX

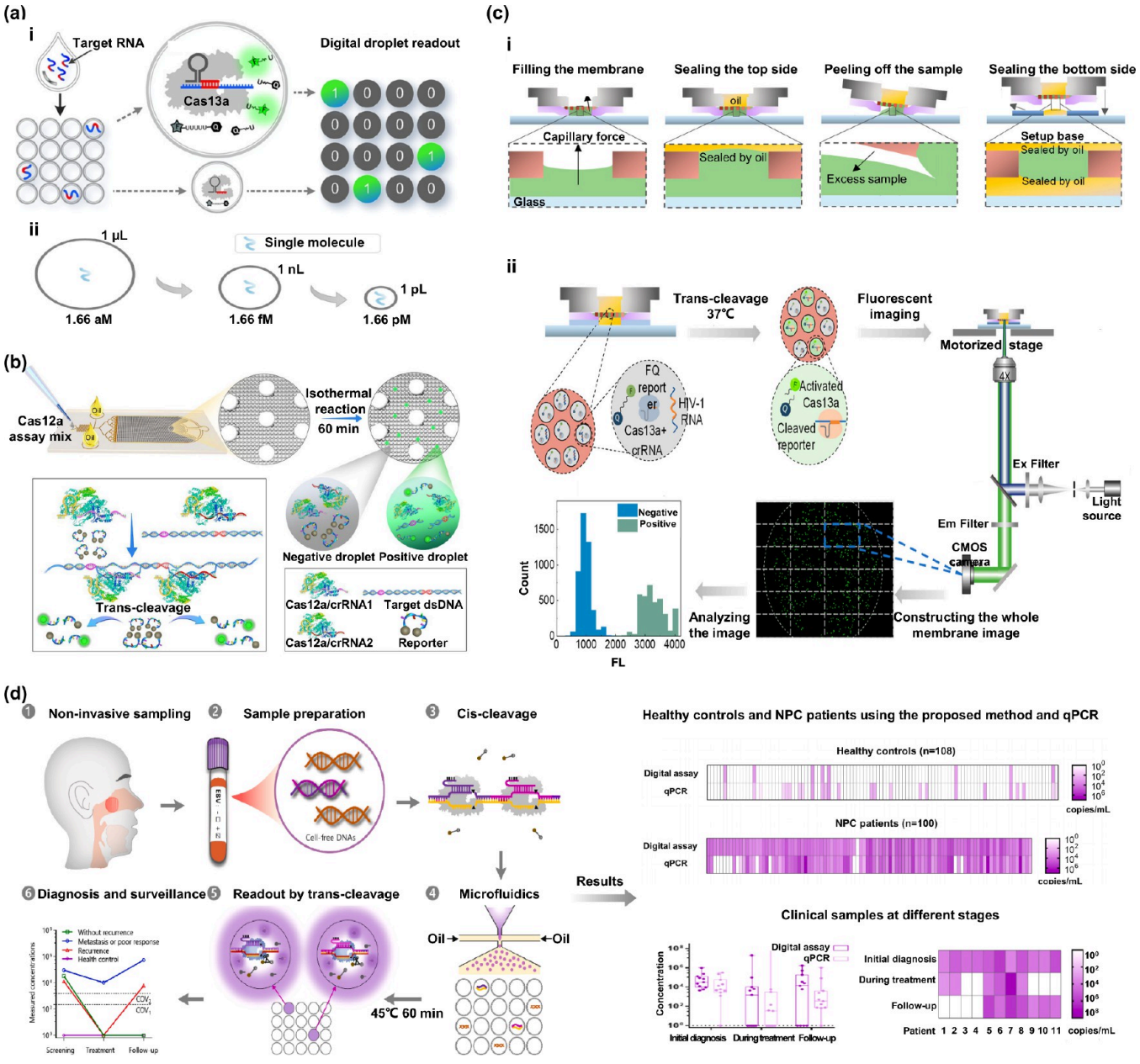


Figure 6. CRISPR-based amplification-free digital sensing was performed with droplet microfluidic chips. (a) Schematic diagram of ultralocalized Cas13a biosensor for RNA detection. Adapted with permission from ref 57. Copyright 2021, American Chemical Society. i: Concept of ultralocalized Cas13a assay; ii: Confinement effect on the local concentration. (b) Schematic diagram of ultralocalized Cas12a biosensor for DNA detection. Adapted with permission from ref 55. Copyright 2021, American Chemical Society. (c) Schematic diagram of STAMP-CRISPR biosensor based on self-digitization automated partitioning through commercial polycarbonate track etch membrane. Adapted with permission from ref 54. Copyright 2023, American Chemical Society. i: STAMP process; ii: Utilization of the STAMP device and CRISPR assay for HIV-1 quantification. (d) Schematic diagram of the double crRNA-mediated CRISPR/Cas12a biosensor for plasma EBV DNA quantification based on QX200 droplet system. Adapted with permission from ref 41. Copyright 2023, Elsevier.

results. The platform reduces detection time to 30 min at 37 °C. However, the separation of amplification and detection into two stages remains a challenge. Droplets must be transferred to a 40-μm-high PDMS chamber via tubes for quantitative monitoring, which increases the false-positive rate and complicates workflow integration. This limits full automation and hinders the practical application of CRISPR digital detection systems in POCT.

To achieve an *in situ* CRISPR digital microfluidic system, Lu et al. ingeniously constructed DMF-Cas12a system based on the synergistic effect of immunomagnetic bead enrichment, nucleic acid amplification, and the CRISPR/Cas12a system to achieve highly sensitive detection of pathogens. (Figure 5d).[40] Unlike the pressure-driven fluid system, the DMF-Cas12a system uses EWOD technology. This approach uses a computer to apply continuous potentials to an electrode array, enabling independent control over RPA amplification, cell lysis, and Cas12a trans-cleavage within droplets. EWOD technology allows for precise droplet manipulation without the need for pipelines, offering high reconfigurability and automation. The system also incorporates magnetic bead-based pre-enrichment, enhancing the sensitivity of *S. aureus*

https://doi.org/10.1021/acsnano.5c03474
ACS Nano XXXX, XXX, XXX−XXX

detection with the LOD of 32 CFU/mL in just 55 min, using only 6.6 μL reagent. Compared to traditional PCR, the sensitivity is improved by 2−3 orders of magnitude and the detection time is drastically reduced, greatly increasing efficiency. The method performs exceptionally well with complex biological samples, such as milk and urine, achieving analytical recoveries of 88.2% to 109% for spiked samples, with coefficient of variation (CV) values below 15%. This demonstrates its potential for automated, highly sensitive pathogen detection in diverse biological applications, including scenarios such as simulated urinary tract infections and food contamination testing. This assay integrates amplification, cell lysis, and detection processes, overcoming the traditional two-step detection model of RPA/LAMP-CRISPR. However, the preenrichment step, where immunomagnetic beads are mixed with the sample on a spinner for 20 min, is not integrated into the digital chip. Instead, centrifugation is required to collect the immunomagnetic beads with the enriched sample before loading them onto the chip. A key area for future advancement in CRISPR digitization is the development of a simple, user-friendly integrated module.

Recent studies have aimed to simplify the CRISPR digitization process. Rolando et al. utilized a commercially available microfluidic chip for real-time digital LAMP.[92] Lin et al., by using easily accessible membranes, conducted LAMP digitization experiments without the need for complex chip fabrication or specialized equipment.[93] Notably, Luo et al. developed a droplet digital hyperbranched amplification-enhanced CRISPR/Cas12a-based telomerase detection platform (ddHECTelo) to detect telomerase activity, skillfully applying a vortex technique without relying on a microfluidic device. (Figure 5e).[53] In this system, Cas12a combines with crRNA to form a complex. When the complex recognizes the TTAGGG-rich DNA sequence extended by telomerase, Cas12a is activated. Subsequently, it cleaves single-stranded DNA reporters, separating the fluorescent and quenching groups and generating a signal. The experimental steps are as follows: First, telomerase was extracted and used to add repeat sequences to the TS primer. Then, a reverse primer initiated hyperbranched amplification, increasing the amount of relevant DNA. The reaction mixture was vortexed for one s to form droplets. After different crRNAs were designed and compared (selecting crRNA2 for its high efficiency) and the reaction conditions were optimized, the fluorescence signals from the droplets were measured. Finally, telomerase activity was accurately quantified based on the number of fluorescent droplets. This method can detect telomerase activity at a level as low as 0.6 MCF-7 cells/μL. Compared with the traditional CRISPR system, ddHECTelo can detect low-abundance target nucleic acids and features a simplified operation. In comparison to PCR, the digital system of ddHECTelo is 10,000 times more sensitive. What makes ddHECTelo unique is its simple droplet-forming process and the incorporation of a hyperbranched amplification. However, to ensure the method's reliability, the uniformity of the droplets during the vortexing process needs to be further regulated. This investigation is crucial for achieving accurate and straightforward quantification in precision medicine.

As illustrated in Figure 4−5, and Table 1, digital CRISPR microfluidic platforms with amplification offer significant advantages over traditional PCR and CRISPR methods. These platforms achieve exceptionally high sensitivity with detection limits in the aM to fM range and are capable of handling diverse sample types. Cas12, a thermophilic RNA-guided endonuclease, is often paired with LAMP for amplification. Compared with LAMP-CRISPR platforms, those incorporating RPA can achieve faster detection. For example, the ddRECD platform requires 120 min for detection, while the PADLOCK platform completes the process in just 30 min. However, current amplification-based strategies have notable limitations. They are time-consuming, involve complex manual operations, and are prone to false positives due to nonspecific activation, which restricts their applicability in clinical diagnostics and biological analysis. To address these challenges and enhance detection sensitivity, it is essential to optimize both microfluidic chips and the CRISPR system. One promising approach is to explore Cas effector proteins further and refine the design of crRNA or gRNA to improve CRISPR sensing capabilities.[94,95] Additionally, developing integrated chips that combine sample pretreatment with CRISPR detection can significantly reduce contamination risks, enhance portability and controllability, and drive advancements in related fields.

3.2. Amplification-Free Strategy. According to the reported literature,[96−100] the use of multiple crRNAs, sensitive readout systems, high-cleavage-activity Cas proteins, and reaction digitization makes it possible to construct amplification-free biosensors, which help balance the sensitivity and specificity of CRISPR technology.

The ultralocalized Cas13a platform developed by Tian et al. allows for ultrasensitive detection (6 copies/μL) without nucleic acid amplification (Figure 6a).[57] It mainly relies on increasing the local molecular concentration and using the efficient Cas13a system. The droplet microfluidic biochip is cleverly designed with a sample inlet, two oil inlets, and an outlet connected to a syringe. In experiments, mineral oil is filled into the chip first, followed by the Cas13a reaction mix. Pressure differences and the chip's flow-focusing structure generate a uniform monolayer of droplets. These droplets contained all reaction components: target RNA, Cas13a, crRNA, and fluorescent RNA reporters. Then, the droplets are incubated at 37 °C. If target RNA is present, it binds to crRNA, activating Cas13a to cleave the fluorescent reporters and emit a signal. The reaction occurs in the chip's tiny, independent droplets, avoiding interference and ensuring reliable results. Compared with traditional RNA detection methods like RT-PCR, the ultralocalized Cas13a platform does not require amplification or reverse transcription, thus avoiding issues like amplification bias, cross-contamination, and sample loss. Compared with bulk Cas13a assays, it is over 10,000 times more sensitive. It can precisely distinguish homologous miRNA sequences and quantify various RNA molecules in different samples, such as microRNAs, 16S rRNAs, and SARS-CoV-2 RNA in cell-line samples, clinical serum, and nasopharyngeal swabs. When detecting miRNA-17 in complex samples, its results are similar to qRT-PCR and ddPCR, but they show a slightly higher miRNA-17 level due to bypassing reverse-transcription problems.

Using the same biochip, Yue et al. developed the ultralocalized Cas12a platform for single-molecule-level DNA quantification without amplification (Figure 6b).[55] Generally, Cas12a was less efficient than Cas13a in trans-cleavage. Thus, the platform uses a dual-crRNA targeting strategy and focuses on screening the optimal reaction parameters of an efficient Cas12a assay. Just by optimizing these parameters, the LOD of this assay can reach 100 fM DNA, which is 50 times more

https://doi.org/10.1021/acsnano.5c03474
ACS Nano XXXX, XXX, XXX−XXX

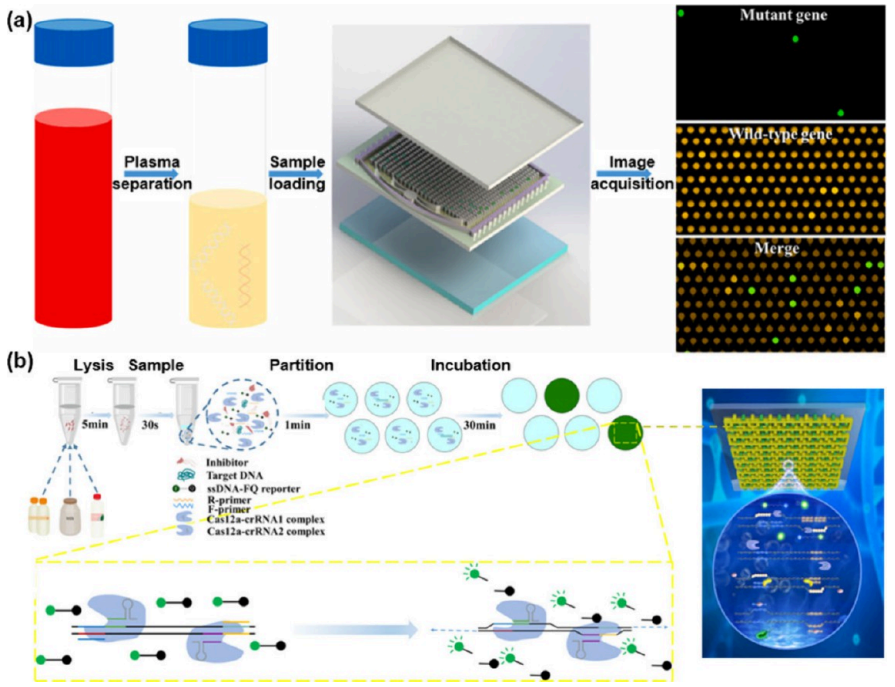


Figure 7. CRISPR-based amplification digital sensing with homemade microarray chips. (a) Schematic diagram of sample loading based on self-priming liquid-dispensing digital microarray chip. Adapted with permission from ref 82. Copyright 2021, Elsevier. (b) Schematic diagram of direct digital dual-crRNA assay method in microarray chip's (a) positive microchamber. Adapted with permission from ref 62. Copyright 2023, American Chemical Society.

sensitive than the traditional Cas12a assay. Based on this, the ultralocalized Cas12a platform with comprehensive optimizations shows superior performance. It can accurately quantify African Swine Fever Virus (ASFV) DNA with an LOD of 17.5 copies/μL. The reaction occurs at 37 °C, and the detection time is 60 min, making it easy to carry out. The flexible programmability of crRNA in the biosensor holds great potential in constructing quantitative analysis tools for DNA.

To expedite the CRISPR/Cas digitization process, Nouri et al. developed a self-digitization approach using the Automated Membrane-based Partitioning (STAMP) for amplification-free detection of HIV-1 with the LOD of 1 fM in less than 30 min (Figure 6c).[54] A commercial PCTE membrane was used in the STAMP platform to create droplets, which has a simple 4-step operation process. Cas13a forms a complex with crRNA, and when it binds to the specific HIV-1 RNA target, it activates and performs trans-cleavage on the FQ-labeled single-stranded reporter, generating a fluorescent signal. By surface tension-induced capillary action, the mixture is pushed into the membrane's pores, which are extremely dense with uniformly sized holes. A sealed digital system is created when the STAMP is positioned on a mineral oil-filled surface, the sample is kept in place by surface tension and it only takes 8 μL of the sample to fill. This platform constructs a simple amplification-free platform, eliminating the need for sophisticated instruments and intricate microarray construction. Compared with traditional RT-qPCR, the detection results of STAMP platform are highly consistent. However, it is limited in detecting low-positive samples (plasma viral load <2000 copies/mL) due to subsampling errors. Despite this limitation, the STAMP-dCRISPR platform shows great potential for clinical applications. In the future, its overall performance can be enhanced in three aspects: improving sensitivity (by increasing sample volume, reducing reaction volume, preconcentrating samples, and using multiple membranes for detection), standardizing operations (by developing an automated membrane filling system), and expanding the dynamic range (by optimizing membrane pore parameters).

To increase the amplification-free CRISPR method's detection effectiveness, Jiang et al. employed CRISPR/Cas12a-crRNA duplexes with the commercial QX200 droplet system for the detection of Epstein−Barr virus (EBV) DNA, targeting the repetitive *Bam*HI−W region of the EBV genome (Figure 6d).[41] The assay leverages the cis-cleavage activity of Cas12a to fragment EBV DNA before droplet generation, increasing the number of detectable targets by 5−11 times depending on the repeat number. The fragmented DNA is then compartmentalized into picoliter-sized droplets, where activated Cas12a-crRNA complexes cleave fluorescent reporters, generating a digital signal for quantification. This approach eliminates the need for preamplification, reducing amplification bias and contamination risks. The assay demonstrated superior sensitivity (99.0%) and specificity (92.6%), outperforming conventional qPCR, particularly in detecting low EBV DNA loads and early stage nasopharyngeal carcinoma (NPC), with an AUC of 0.9883. A key strength of this assay lies in its use of double crRNA-mediated cis-cleavage, which eliminates the need for Cas protein activity or highly complex micronano fabrication technologies, thereby enabling amplification-free detection. It also verified that digital CRISPR biosensors can be integrated with commercial systems to enhance detection stability and practicability. The amplification-free design, coupled with its absolute quantification capability, simplifies standardization across testing centers, positioning it as a promising alternative to PCR-based methods for NPC management.

Compared with traditional PCR and amplification-based CRISPR platforms, CRISPR-based digital microfluidic plat-

https://doi.org/10.1021/acsnano.5c03474
ACS Nano XXXX, XXX, XXX−XXX

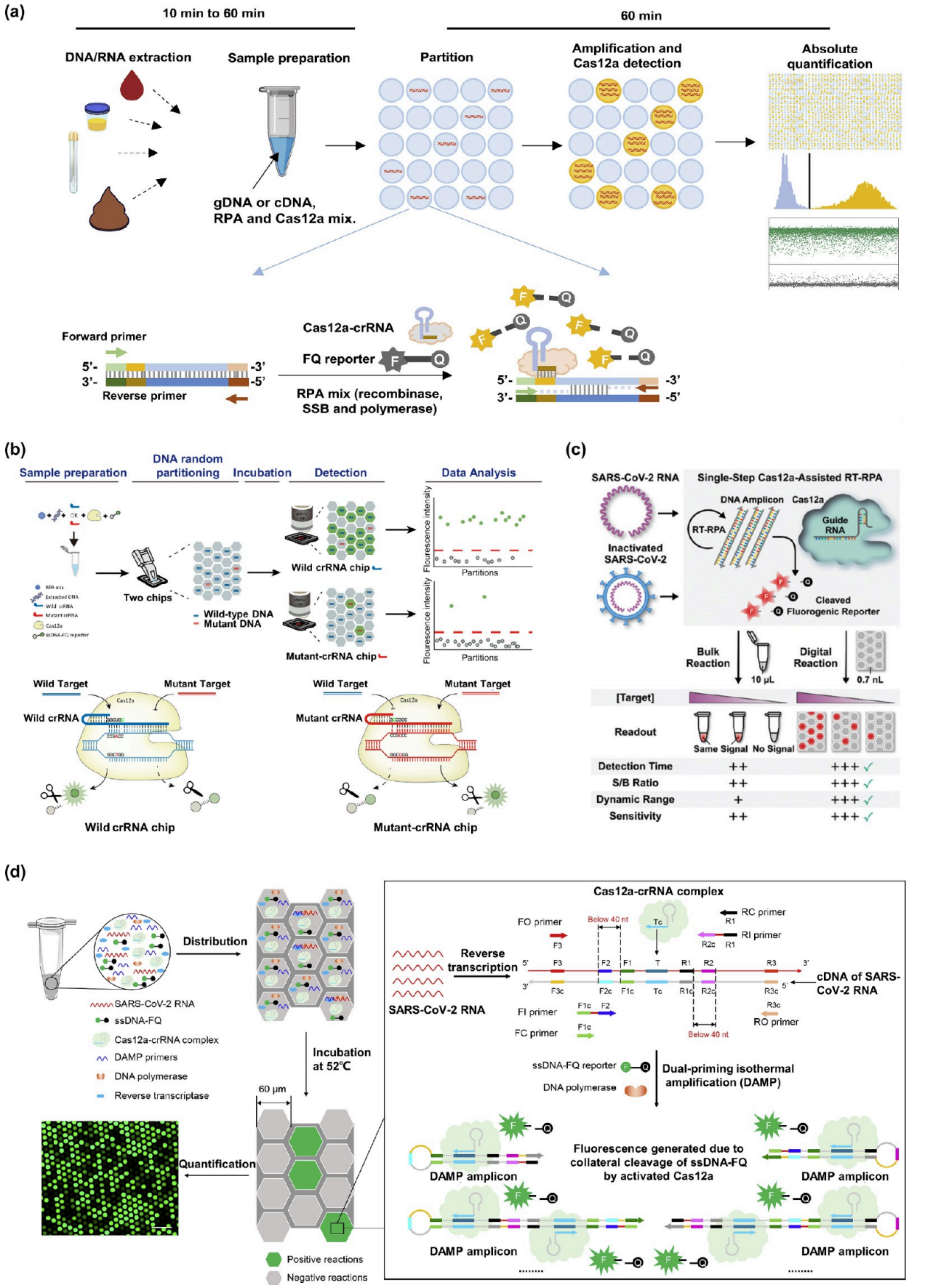


Figure 8. CRISPR-based amplification digital sensing with commercial microarray chips such as the QuantStudio digital chip and Clarity digital chip. (a) Schematic diagram of rapid digital CRISPR approach (RADICA) based on one-pot RPA-CRISPR/Cas12a and Clarity digital

https://doi.org/10.1021/acsnano.5c03474
ACS Nano XXXX, XXX, XXX−XXX

Figure 8. continued

chip. Adapted with permission from ref 36. Copyright 2021, Elsevier. (b) Schematic diagram of CASMART biosensor for precise quantitative detection of rare mutant alleles based on one-pot RPA-CRISPR/Cas12a and Quantstudio 3D digital chip. Adapted with permission from ref 63. Copyright 2022, Elsevier. (c) Schematic diagram of deCOViD biosensor for SARS-CoV-2 quantitative detection based on one-pot RPA-CRISPR/Cas12a and Quantstudio 3D digital chip. Reprinted with permission under a Creative Commons CC-BY 4.0 License from ref 37. Copyright 2021, Wiley. (d) Schematic diagram of dWS-CRISPR biosensor for SARS-CoV-2 quantitative detection based on one-pot RT-DAMP-CRISPR/Cas12a and Quantstudio 3D digital chip. Adapted with permission from ref 60. Copyright 2021, Elsevier.

forms without amplification have a shorter detection time, requiring only 30 to 60 min (Table 1). These platforms achieve single-molecule sensitivity, enabling absolute quantification of DNA and RNA without the need for preamplification, thus avoiding issues such as amplification bias, cross-contamination, and sample loss.[31,32,101] Moreover, the droplets used in these platforms are all in the picoliter range, which helps to further enhance the detection sensitivity. Compared with amplification strategies, the reaction temperature of amplification-free strategies is always 37 °C, which enables the realization of numerous application scenarios. However, challenges remain, including the need for further optimization of reaction conditions and droplet readout techniques to improve multiplexing capabilities and detection robustness. Future advancements in CRISPR-based droplet assays could focus on integrating sample preparation steps, enhancing crRNA design, reducing the reaction time, and developing portable detection systems to expand their applicability in point-of-care diagnostics and large-scale screening.

4. DIGITAL CRISPR BIOSENSORS BASED ON MICROARRAY CHIPS

Droplet-based digital CRISPR technology has been developed to identify RNA and DNA, *etc.*[64,102−105] It takes some time for the droplet's reaction time to identify the fluorescence signal of a single droplet. In addition, factors such as surface tension might hinder droplet stabilization in the detection process. Compared with microdroplets, microarrays are produced using soft etching and have a more uniform size. It is expected that microarray chips will reach even higher sensitivity and more precise detection. Thus, this section analyzes the performance of the digital microarray CRISPR technology, both amplification-based and amplification-free. Specifically, the combination strategies, strength, and potential applications.

4.1. Amplification Strategy. Xia et al. developed a self-priming digital PCR microarray chip with rapid sampling, precise quantification, low evaporation, and power-free operation (Figure 7a).[82] The biochip is composed of three layers: glass, microstructure, and a Scotch-tape-based adhesive layer for preventing evaporation. The 20160 cylindrical microchambers allowed for independent PCR amplification. The pressure difference between the chip's inside and exterior causes it to draw in the reaction solution. The chip can detect the epidermal growth factor receptor (EGFR)T790 M mutation in plasma with 100% accuracy and 0.01% sensitivity, simplifying the workflow and boosting the detection efficiency. Using this self-priming digital chip, a direct digital dual-crRNAs assay (3D assay) was proposed to precisely quantify pathogens (Figure 7b).[62] The chip features a hydrophilic modification to prevent protein adsorption, enabling one-pot RPA amplification and CRISPR/Cas12a detection on a single microarray platform. *Salmonella* could be detected within 30 min with a LOD of 0.2 cells/mL in the range of 2.58×10^1 to 2.58×10^4 cells/mL. This platform overcomes the limitations of traditional two-step CRISPR assays and protein adsorption issues in microfluidic chips, offering a robust solution for rapid and accurate pathogen detection.

Many commercial microarray chips, such as QuantStudio and Clarity chips, are used to accelerate the CRISPR/Cas digitization process. Wu et al. integrated isothermal amplification, CRISPR/Cas12a detection, and digital PCR partitioning to develop RADICA (Figure 8a).[36] In RADICA, RPA amplifies the target nucleic acid and the Cas12a-crRNA complex specifically binds and cleaves the target, generating a fluorescent signal. A single reaction mixture was partitioned into tens of thousands of compartments on the high-density chip, with an average volume of 1.336 nL. RADICA can quantify nucleic acids in 40−60 min, four times faster than dPCR-based detection. RADICA can detect SARS-CoV-2 in the linear dynamic range of 0.6−2027 copies/μL ($R^2 > 0.99$), showing high accuracy, low variability, negligible cross-reactivity to similar targets, and high tolerance to human background DNA. It can be combined with reverse transcription for RNA quantification and is customizable for other amplification platforms and Cas proteins. Based on the same chip, the Warm-Start RApid DIgital CRISPR Approach (WS-RADICA) based on RT-LAMP was proposed to detect SARS-CoV-2 in 60 min with a LOD of 1 copy/μL,[61] which prevents amplification at room temperature before sample loading and enables accurate digital quantification.

Previous studies have mainly focused on nucleic acid and bacterium detection. The rapid spread of diseases like COVID-19 is directly related to early mutations in the SARS-CoV-2 viral genome, which alters its structure. Thus, prompt and reliable mutant gene detection is crucial for limiting viral transmission. For accurate mutant allele quantification, Zhang et al. integrated RPA and CRISPR/Cas12a trans-cleavage to develop the CASMART platform (Figure 8b).[63] A commercial QuantStudio 3D Digital PCR Chip was used to partition the reaction mixture into ∼20,000 microwells for digital detection. In CASMART, RPA amplifies the target nucleic acid, and the Cas12a-crRNA complex specifically binds to and cleaves the target, triggering the trans-cleavage of the ssDNA-FQ reporter and generating a fluorescence signal. LbCas12a, AsCas12a and their variants were selected for the CASMART platform due to their different sensitivities to gRNA-target substrate incomplete base pairing. Mutant crRNA2 and wild-type crRNA6 were selected for subsequent cleavage studies to find rare mutant alleles due to their strong target sensitivity and weak nonspecific fluorescence signals. This platform can accurately quantify the variant allele frequency of EGFR L858R within 60 min at 42 °C and detect mutant targets as low as 0.3 copies/μL (0.498 aM) in mock multiplex cfDNA samples. Compared with Next Generation Sequencing (NGS), the CASMART platform shows good concordance in quantifying mutant alleles in human genomic samples.

Utilizing the same commercial microarray chip. Park et al. developed a one-pot digital RPA-CRISPR/Cas12a platform

https://doi.org/10.1021/acsnano.5c03474
ACS Nano XXXX, XXX, XXX−XXX

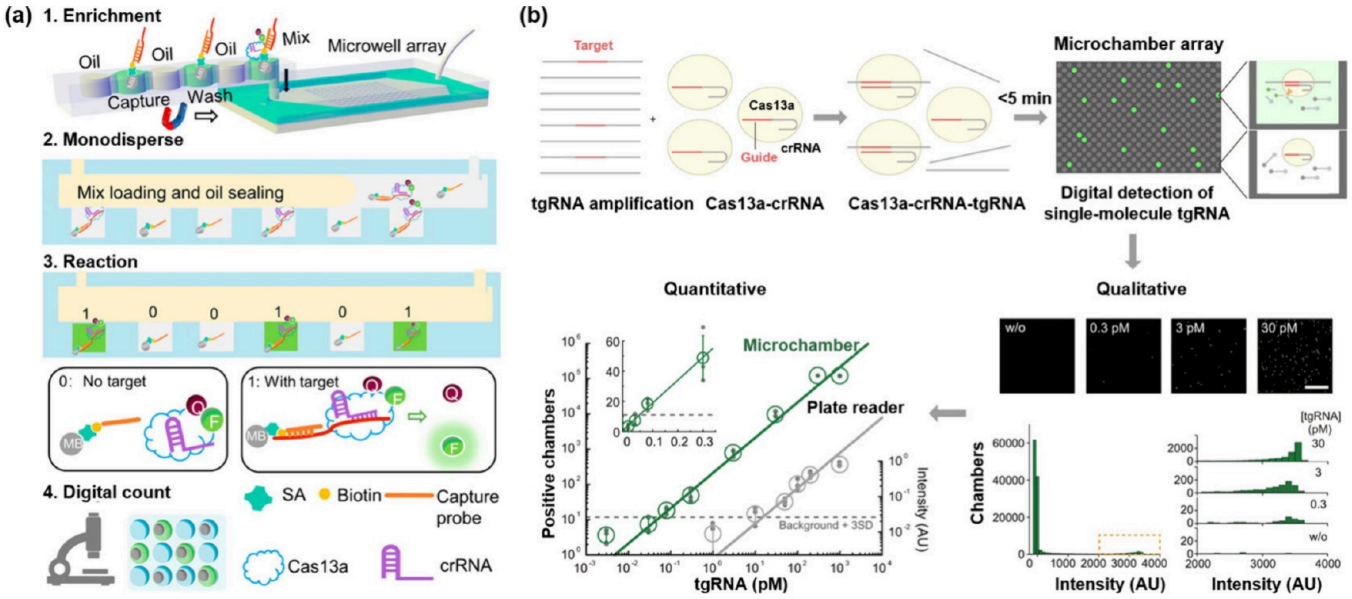


Figure 9. CRISPR-based amplification-free digital sensing was performed with microarray chips. (a) Schematic diagram of high-integrated microwell array and magnetic-bead-based dCRISPR biosensor. Magnetic beads are used to extract and enrich targets from large sample volumes, achieving the integration of sample pretreatment and detection. Adapted with permission from ref 38. Copyright 2023, American Chemical Society. (b) Schematic diagram of ultrarapid SATORI biosensor based on fL-level microchambers and the strong cleavage activity of LwaCas13a. Reprinted with permission under a Creative Commons CC-BY 4.0 License from ref 64. Copyright 2021, Springer Nature.

called deCOViD (Figure 8c).[37] In deCOViD, SARS-CoV-2 RNA or heat-inactivated SARS-CoV-2 is reverse transcribed and amplified by RT-RPA. The resulting DNA amplicons activate Cas12a-guide RNA complexes, which cleave single-stranded DNA fluorogenic reporters to produce fluorescence. This allows deCOViD to achieve qualitative detection in <15 min and quantitative detection in 30 min, with high sensitivity down to 1 genome equivalent (GE)/μL of SARS-CoV-2 RNA and 20 GE/μL of heat-inactivated SARS-CoV-2. In detecting heat-inactivated SARS-CoV-2, deCOViD can directly detect samples without RNA extraction and shows a 5-fold improvement in sensitivity compared to the bulk assay. However, neither RADICA nor deCOViD resolves the challenge of overestimating the initial targets induced by the RPA. Because RPA could be initiated at room temperature. The reaction assay must be prepared on ice and loaded into chips within 1 min, which complicates the detection procedure and remains difficult in massive testing applications. Ding et al. developed the digital warm-start CRISPR (dWS-CRISPR) platform by integrating RT-DAMP and CRISPR/Cas12a detection to tackle issues like premature target amplification and false positives (Figure 8d).[60] Using the same QuantStudio 3D digital chip, the reaction mixture was partitioned into over 10,000 subnanoliter microreactions. In the dWS-CRISPR assay, six RT-DAMP primers recognize target sequences to initiate nucleic acid amplification. Subsequently, the Cas12a-crRNA complex binds to the amplicons, activating the collateral cleavage activity that cleaves ssDNA-FQ reporters and generates fluorescence. This assay can detect down to 5 copies/μL SARS-CoV-2 RNA in the chip and was clinically validated on 32 clinical swab samples and 3 clinical saliva samples. It can also directly detect SARS-CoV-2 in heat-treated saliva samples without RNA extraction. The dWS-CRISPR platform is efficiently initiated at 50−55 °C, preventing premature amplification at room temperature. This platform offers high specificity and is 10 times more sensitive than traditional tube-based bulk assays.

RPA, LAMP, DAMP, *etc.* are always used in microarray-based digital CRISPR biosensors to enhance detection sensitivity. In addition, commercial digital chips are always used to eliminate manual steps and reduce operational errors. Compared to microfluidics-based CRISPR biosensors, microarray-chip-based CRISPR biosensors have a lower LOD in the aM range, and their microchambers have a larger volume than droplets. The detection time for these biosensors typically ranges from 30 to 90 min, and the dWS-CRISPR has a relatively long detection time of 90 min. Future improvements for microarray-chip-based CRISPR biosensors include exploring new adaptive digital chips, optimizing reagent concentrations, enhancing user-friendliness, replacing fluorescence microscopy with mobile phone-based detection for portability, and applying it to study the relationship between SARS-CoV-2 viral load and the COVID-19 state and to detect other diseases.

4.2. Amplification-Free Strategy. From the perspective of sample pretreatment, Wang et al. created the dCRISPR platform based on high-integrated microarray chips and magnetic beads-integrated CRISPR/Cas13a to avoid amplification process (Figure 9a).[38] Sample pretreatment is the most difficult step in nucleic acid testing since it involves complex processes, such as sample lysis, nucleic acid extraction, and purification. Magnetic beads are used to extract and enrich RNA from large sample volumes, allowing for less aerosol contamination. The complete process takes less than 50 min, which is shorter than most CRISPR/Cas systems and PCR systems combined. Moreover, the distribution and limitation of the target-induced CRISPR/Cas13a cleavage reaction to one million unique femtoliter-sized microwells enhance the local signal intensity and allow SARS-CoV-2 detection at the extremely detection limit of 2 aM without the requirement for single-molecule amplification.

https://doi.org/10.1021/acsnano.5c03474
ACS Nano XXXX, XXX, XXX−XXX

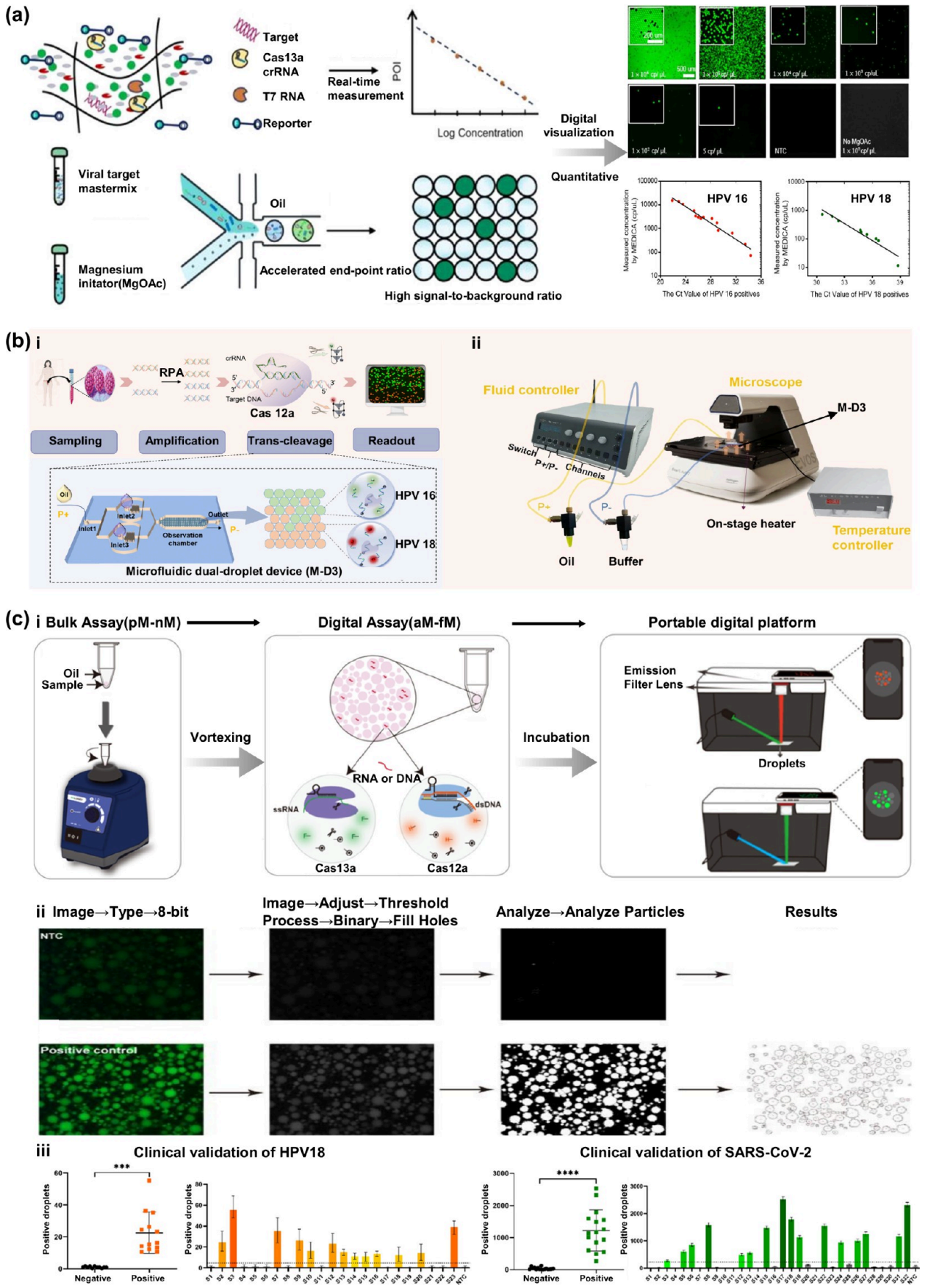


Figure 10. Digital CRISPR sensing applications in multigene detection based on droplet microfluidic chips. (a) Schematic diagram of the MEDICA biosensor for HPV16 and HPV18 detection based on RPA-CRISPR one-pot reaction. Adapted with permission from ref 56.

https://doi.org/10.1021/acsnano.5c03474
ACS Nano XXXX, XXX, XXX−XXX

Figure 10. continued

Copyright 2022, American Chemical Society. (b) Schematic diagram for stimulation detection of HPV 16 and HPV 18 based on an integrated dual-droplet device called M-D3.[59] i: Working principle of the M-D3; ii: Dual-droplet microfluidic platform setup. Adapted with permission from ref 59. Copyright 2023, American Chemical Society. (c) Schematic of the PddCas biosensor for amplification-free dual-gene detection based on vortex-assisted droplet generation. Adapted with permission from ref 58. Copyright 2023, American Chemical Society. i: The detection process with the portable digital platform; ii: Data processing to quantify the number of positive droplets; iii: Clinical validation of HPV 18 and SARS-CoV-2.

To further achieve the ultraquick detection of RNA, Makino et al. created the CRISPR digital microarray biosensor called SATORI, which does not require amplification (Figure 9b).[64] Utilizing fL-level microchamber and robust cleavage activity of LwaCas13a (k = 1.1 × 10^7 × [FQ rep.] $M^{-1}s^{-1}$), SATORI achieved massively parallel monitoring of chemical reactions at the single-molecule level in just 5 min at 37 °C. SATORI's detection efficiency is highly attractive, considering its $9.10 cost ($5.20 for the microchamber and $3.90 for the reagents). Containing more than 1 × 10^6 microchamber, it is a quick and efficient diagnostic tool with a LOD of 5 fM. From the biosensor of dCRISPR and SATORI, reducing the microchamber volume and promoting sample pretreatment efficiency is suggested to further minimize the detection limit or response time.

The development of microarray chips has significantly advanced CRISPR-based digital sensing technologies, driving progress in healthcare and related fields. Among the CRISPR digital biosensors discussed, the SATORI platform demonstrates the fastest detection capability, achieving results in just 5 min. However, its detection sensitivity remains relatively limited at 5 fM. Optimizing the microchamber volume could potentially improve this sensitivity. Compared with the CRISPR droplet microfluidic biosensor, the digital CRISPR biosensors based on microarray chips have a faster initial detection speed, since it does not necessitate the creation of droplets. Because there are fewer reaction channels in the microarray approach, it saturates at high concentrations, resulting in a linear range shorter than that of the droplet microfluidic biosensor. Consequently, the two techniques can cooperate to yield better detection results.

5. DIGITAL CRISPR SENSING APPLICATIONS IN MULTIGENE DETECTION

Technologies utilizing digital CRISPR biosensing are renowned for their high sensitivity and specificity in detection. However, the CRISPR/Cas system is nonspecific for the trans-cleavage of reporter genes, making it difficult to distinguish signals in situations with multiple targets. As a result, multiple target detection is not a suitable use for the CRISPR digital biosensors discussed above, which are primarily intended for single target identification. Ideal diagnostic and monitoring technologies should be highly multiplexed and easily scalable to hundreds of samples to detect multiple viruses, distinguish between viral variants, and quantify viral load.[65,106−110] The intersection of CRISPR technology with droplet microfluidics and microarray chips for multiplexed detection is thus summarized in this section. It also explores the opportunities and development of digital CRISPR multiplexed detection technology, focusing on mutual interference, sensitivity, specificity, and sensitive element recognition mechanisms.

5.1. Multigene Detection Based on Droplet Microfluidic Chips. By altering the crRNA or tracrRNA in the CRISPR/Cas system, most previous studies have employed the same Cas mechanism to target multiple sequences.[31,106,111,112] While this approach simplifies signal interpretation, it also necessitates separate assays and extends detection time. An alternative approach involves using multiple CRISPR/Cas proteins in a single assay, such as combining Cas12a and Cas13a or utilizing the four enzymes of LwaCas13a, PsmCas13b, CcaCas13b, and AsCas12a.[113,114] The aforementioned orthologous Cas proteins are introduced together with nucleic acid reporters that are modified with different fluorophores to accomplish this. Each Cas mechanism will cleave the matching reporter labeled with a particular fluorophore. This is feasible, but expensive multichannel fluorescence detectors and screening of Cas proteins are required. Utilizing the unique features of droplet microfluidic devices, such as parallel sample processing and multianalysis integration, multiple detection can be achieved by dividing up the Cas protein/crRNA reaction solutions for different targets among the various microcavities.

Achieving ideal one-step multiplexed detection addresses macromolecular crowding and enzymatic incompatibility to achieve comparable performance to the two-step method. In the RPA-CRISPR one-pot reaction, local reagent depletion will occur in the Cas13a reaction if the RPA reaction mixture is added to the system without sufficient diffusion or mixing. Liu et al. demonstrated that reducing the concentration of PEG-8000 could alleviate the crowding effect and improve the reproducibility of one-pot reactions (Figure 10a).[56] Additionally, enzymatic incompatibility was resolved by designing a dual-Y-channel droplet microfluidic device to isolate MgOAc from the target-containing master mixture. This design ensures that the RPA-Cas13a reaction is activated only after the two reagents are mixed within the droplets, preventing premature cleavage of unamplified targets. The technique enhances molecular mobility within the less viscous droplets, facilitating efficient reagent mixing and concentrating the detection signal, thereby improving the overall assay performance.

The designed MEDICA based on the one-pot RPA-CRISPR/Cas13a was utilized for clinical detection of HPV16 and HPV18 within 25 min, which enhanced the CRISPR system's multiple detection process by exploiting the multiplexing property of droplet microfluidics. It is worth noting that approximately 70% of invasive cervical cancers globally are caused by two of the most common and deadly HR-HPV subtypes: HPV16 and HPV18.[115−117] Co-detection for HPV16/18 improves the chance of identifying precancerous cellular structures early and initiating therapy promptly to halt the spread of cancer. It is crucial to consider that employing multistep procedures can increase the risk of contamination and sample loss during the detection phase, as well as make it more difficult to measure the targets precisely. However, in MEDICA, two sets of RPA and Cas13a sequences were designed to enable multiplex detection. Each set was applied to the detection process separately rather than simultaneously.

https://doi.org/10.1021/acsnano.5c03474
ACS Nano XXXX, XXX, XXX−XXX

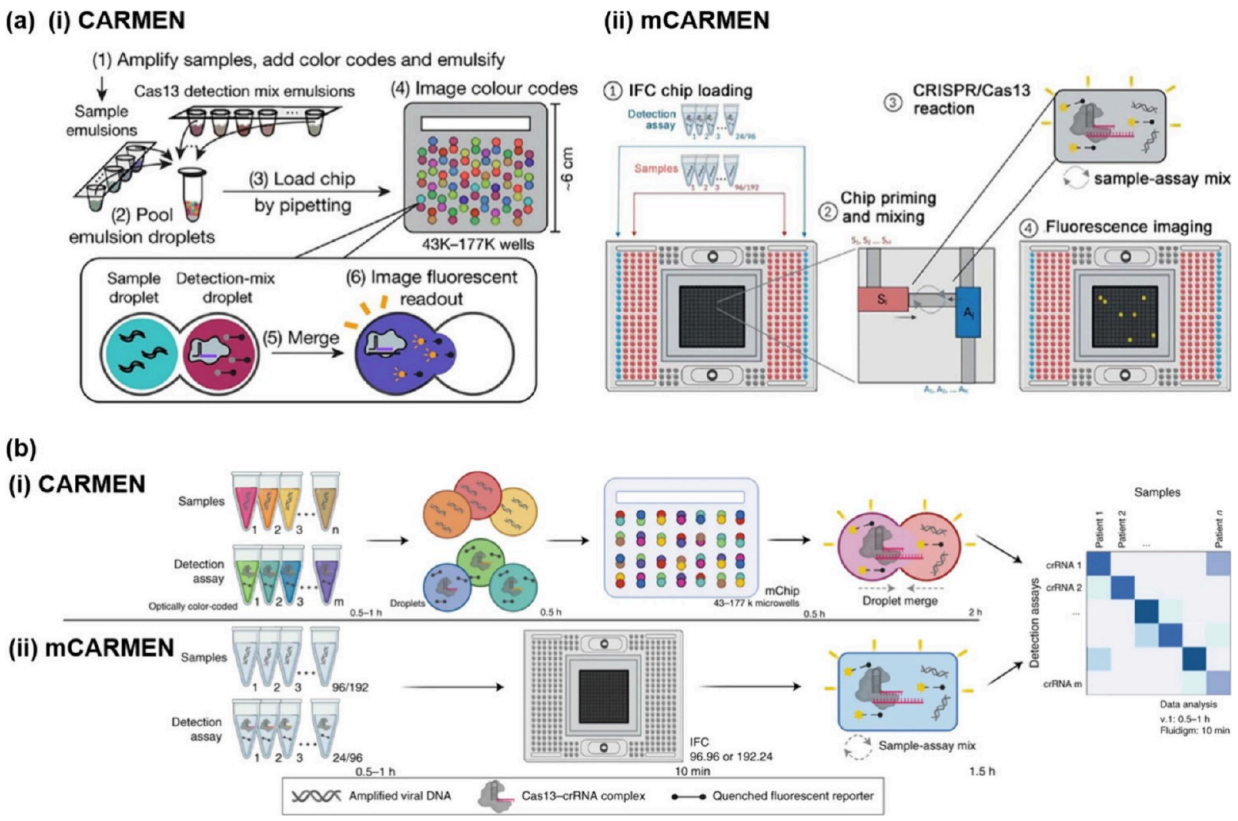


Figure 11. Digital CRISPR sensing applications in multigene detection based on microarray chips. (a) Microarray chip used in CARMEN[80] (i) and mCARMEN[81] (ii), CARMEN and mCARMEN are driven by pairwise combinations of droplets and Fluidigm 192.24 IFC, respectively. (b) (i) Schematic of CARMEN workflows: each amplified sample or CRISPR/Cas13a assay reagent mixture is fluorescently labeled and emulsified to form droplets, respectively. Two droplets are self-organized and merged to activate the CRISPR/Cas13a detection reaction in each well of the chip. (ii) Schematic diagram of mCARMEN workflows: without emulsion and color-coding steps, up to 196 amplified samples and up to 24 detection assay reactions are added to the Fluidigm IFC, respectively. Droplet mixture and CRISPR detection are achieved automated. Reprinted with permission under a Creative Commons CC-BY 4.0 License from ref 80. Copyright 2020, Springer Nature. Reprinted with permission under a Creative Commons CC-BY 4.0 License from ref 81. Copyright 2022, Springer Nature.

To identify multiple targets in one chip simultaneously, Zhao et al. developed the CRISPR-based dual-droplet microfluidic (M-D3), which made it possible to detect HPV16 and HPV18 simultaneously on a single chip (Figure 10b).[59] M-D3 is a two-branch system that efficiently and economically generates two sets of droplets in parallel that contain the fluorescent probes and Cas12a/crRNA, respectively. To differentiate between HPV subtypes based on the fluorescence color of the droplets, EVOS FL Auto 2 imaging equipment and ImageJ software were used for the fluorescence imaging analysis. When paired with RPA amplification, M-D3 can simultaneously detect HPV16 and HPV18 in less than 30 min, with an LOD of 10^{-18} M (1 copy/reaction). After being thermally lysed and amplified, 20 clinical patient samples at risk of HPV infection were classified as positive or negative with 92.3% sensitivity and 100% specificity. The rapid analysis time and few sample consumptions of M-D3 dual-target biosensors make it a promising tool for multiplex nucleic acid detection applications. With its excellent scalability, this digital CRISPR multiplexing technique can be developed into a three-plex or six-plex droplet device to detect multiple targets. Its independent parallel channels and the need for RPA amplification limit further development.

The biosensors described above are all for multiple RNA or DNA detection. Combining Cas12a and Cas13a enables dual-gene detection of DNA and RNA as Cas12a is an enzyme that breaks down DNA and Cas13a is an RNase. Xue et al. developed PddCas, a microarray-free dual-gene technique for DNA and RNA amplification-free detection (Figure 10c).[58] Because of the cleavage preference of CRISPR/Cas, PddCas can detect target DNA and RNA using fluorescent reporter genes matching those of LbaCas12a and LbuCas13a. The mixture of CRISPR/Cas reagents and oil was separated by the vortex mixer spinning at a steady speed of 2500 rpm, resulting in picoliter-scale polydisperse droplets in seconds. PddCas' confinement effect enables it to detect target DNA and RNA in 20 min with LOD of about 100 and 10 aM, respectively. In addition to being about 3×10^4–10^5 times more sensitive than similar bulk CRISPR assays, this also reduces false-positive interference and avoids carry-over contamination. To distinguish positive and negative droplets correctly, the fluorescence image was transformed into a binary representation with the threshold being the mean fluorescence intensity of the NTC plus three times the standard deviation. PddCas has demonstrated 100% sensitivity and specificity in clinical validation using 32 nasopharyngeal swabs for SARS-CoV-2 and 23 cervical epithelial cell samples for HPV 18. Combining a vortex mixer, thermostat, and a homemade portable device with a smartphone, PddCas achieves a portable application with a device cost of less than $400, and reagents cost $0.50 per reaction. It works better for qualitative monitoring and accurately differentiates between the positive and negative

https://doi.org/10.1021/acsnano.5c03474
ACS Nano XXXX, XXX, XXX−XXX

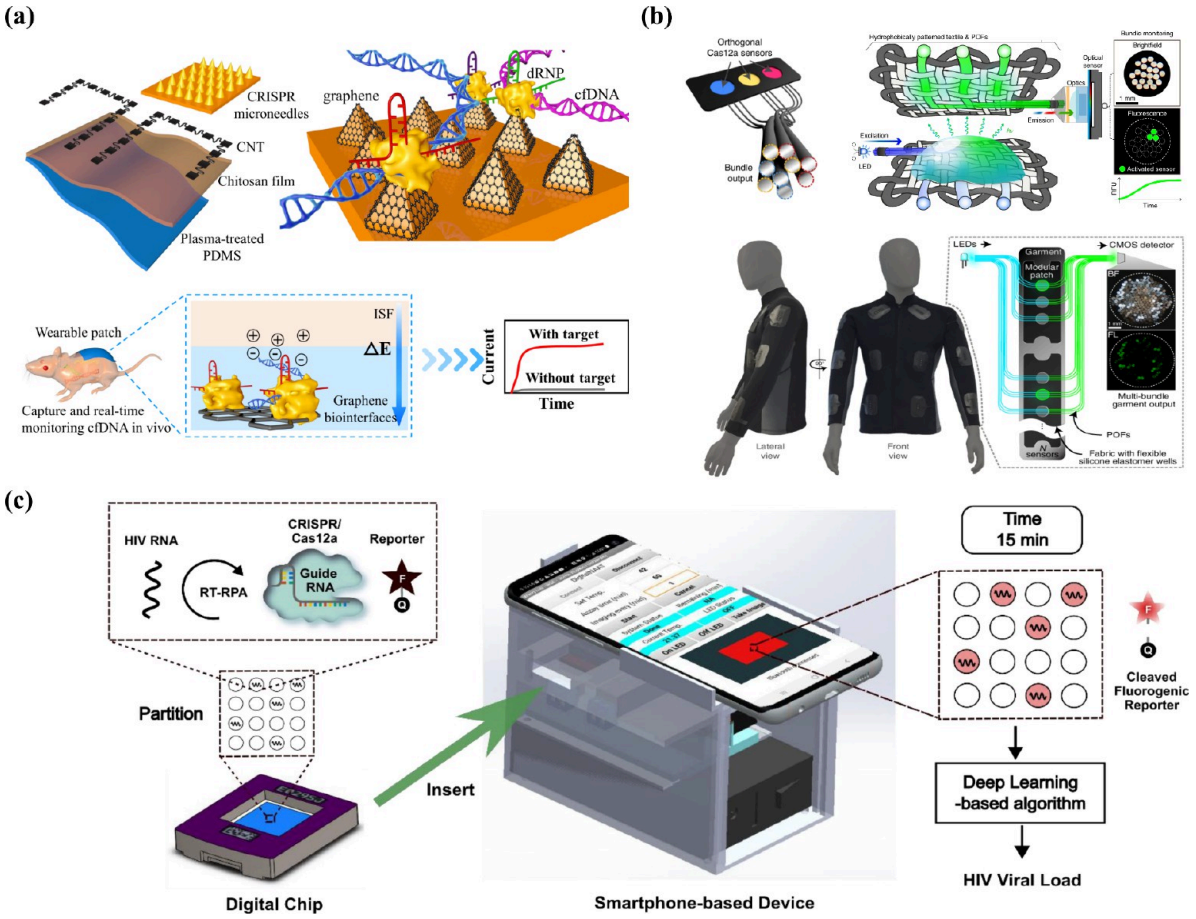


Figure 12. Digital CRISPR sensing applications in wearable technology. (a) CRISPR/dCas9-based wearable microneedle patch for real-time monitoring. Reprinted with permission under a Creative Commons CC-BY 4.0 License from ref 123. Copyright 2022, Springer Nature. (b) CRISPR/Cas12a/Cas13a embedded textiles as wearable biosensors. Adapted with permission from ref 124. Copyright 2021, Springer Nature. (c) Smartphone-enabled digital CRISPR/Cas12a device for rapid and portable quantification of HIV viral load. Adapted with permission from ref 125. Copyright 2024, Elsevier.

samples. The quantification of positive droplets using the improvised portable device demonstrates lower accuracy, compared to that obtained through fluorescent microscopy analysis. Precise quantitative identification requires deep learning techniques and modified statistical models.

The ideal diagnostic should have the monitoring capability to simultaneously process hundreds of patient samples, detect multiple viruses, distinguish between viral variants, and quantify viral loads. Nonetheless, most CRISPR diagnostics only identify one to three targets per sample, which is insufficient for differential diagnosis via comprehensive microbe or variant identification. Other techniques, such as RT-qPCR, are high-throughput and can identify at least 88 samples in a single run but only 1−3 analytes. Multiplex technologies such as Cepheid Xpert Xpress can detect 4 respiratory viruses in up to 16 samples per run, while BioFire can simultaneously detect 22 respiratory pathogens in one sample. Only a few clinical diagnostic techniques are capable of fully detecting the SARS-CoV-2 mutation. However, it is time-consuming and expensive and requires bioinformatic expertise to interpret. The multiple detection capabilities of CRISPR may be further enhanced to overcome the limits above. Thus, interdisciplinary or multitechnology synergies are needed to enhance digital CRISPR sensing.

5.2. Multigene Detection Based on Microarray Chips.

To meet the public health requirements for rapid detection of a wide spectrum of viruses and variants, it is critical to expand the capabilities of CRISPR-based digital biosensors to enable multitarget detection. Ackerman et al. have developed the biosensors called combinatorial arrayed reactions for multiplexed evaluation of nucleic acids (CARMEN)[80] and microfluidic CARMEN (mCARMEN),[81] which are clinically useful surveillance technologies (Figure 11). Microtiter microarrays and CRISPR/Cas13a are used in the CARMEN biosensor for large-scale multiplexed nucleic acid detection. M sample*N crRNAs are utilized to form M*N tests at a time on the chip (4500 statistically repeated tests per chip) without preloaded reagents preloaded. Each amplified sample or CRISPR/Cas13a assay reagent mixture is prepared, fluorescently labeled, and emulsified in fluorine oil to form a 1 nL droplet in a standard microtiter plate. Each microwell in the microarray can hold two droplets at random, allowing droplets of amplified samples and CRISPR/Cas13a detection reagents to self-organize into pairs. An electric field causes the droplet pairs in each microwell to merge, initiating each detection reaction simultaneously. This biosensor, which uses color barcoding, can simultaneously distinguish all 169 viruses associated with humans in a single test and detect the pathogens responsible for the COVID-19 pandemic. CARMEN is practically scalable

https://doi.org/10.1021/acsnano.5c03474
ACS Nano XXXX, XXX, XXX−XXX

due to its built-in multiplexing and throughput capabilities, and its miniaturized design reduces reagent costs per assay by more than 300-fold. It has made it possible for surveillance and diagnostic operations to switch from the focused examination of high-priority samples to the extensive testing of sizable sample sets. Microarray-based, scalable digital CRISPR biosensors have significantly improved patient prognosis and public health. However, they are challenging to apply in clinical due to their high workload (8−10 h) and low-throughput sample examination.

Based on the CARMEN concept, mCARMEN was designed to combine with commercial Fluidigm chips and equipment with a detection time of 140−170 min. For less than $13 per sample, it is possible to simultaneously detect up to 196 preamplified samples and 24 detection assay reactions containing Cas13-crRNA complexes. By utilizing Fluidigm 192.24 integrated with fluidic circuits (IFCs), mCARMEN eliminates the need for color coding and droplet station. Further advancements in public health surveillance are anticipated due to the reduction of manual handling and optimization of the mCARMEN test procedure through the utilization of the commercially available Fluidigm microarray chip, control system, and analytic software.

Compared with the other multiplexing methods, the CARMEN or mCARMEN methodology offers the advantage of high throughput and multiplexing capabilities. mCARMEN has a 100% sensitivity rate, which is higher than the 86% sensitivity rate of CARMEN. With a LOD of 10^2 copies/μL and the ability to detect 192 samples with 24 detection assays simultaneously, mCARMEN is ideal for monitoring multiple viruses and variants. However, the two-step PCR-Cas13a procedure restricts further advancement. mCARMEN might be enhanced by upcoming CRISPR-based amplification-free technologies.

Droplet microfluidics and microarray-based CRISPR digital biosensors can achieve absolute quantification and multiplex detection simultaneously. It solves mutual interference and regulation issues, enabling rapid, high-throughput, and integrated digital detection. Technological developments in micronano machining, 3D/4D printing, and CRISPR amplification-free technology will further enhance precision, reduce costs, and facilitate automation, commercialization, and extensive use of CRISPR-based digital multiplex detection.

6. DIGITAL CRISPR SENSING APPLICATIONS IN WEARABLE TECHNOLOGY

As healthcare reform progresses, wearable technology is rapidly advancing in the field of modern personalized treatment and real-time monitoring.[118,119,22,120] Microfluidics is recognized as a powerful tool for digitizing wearable devices, owing to its superior functional diversity, microscopic scale, and superior mechanical properties.[118,121,122]

CRISPR microfluidics based on microneedles were created to capture and track generic cell-free DNA over an extended period. Skin-piercing hydrogel microneedles were used to harvest and concentrate nucleic acids in tissue fluids by a capillary action. To further improve the real-time monitoring performance, a graphene interface was decorated on the microneedles to enable efficient interactions with charged compounds and electron transport (Figure 12a).[123] Inactivated Cas9 enzyme and single guide RNA (dCas9/sgRNA) were covalently attached to the graphene interface as a driving force for the continuous search and detection of target DNA. However, these approaches inevitably have some limitations. For example, maintaining the viability and functionality of wearable sensing systems based on live cells requires managing temperature and gas levels, removing waste, and supplying nutrients—all of which present technical challenges. Concerns about biocontainment and biohazards may also arise from genetically engineered cells. Expanding the applications of CRISPR-based digital wearable sensing could involve addressing the discrepancy between the practical requirements of wearable devices and the limits of existing CRISPR sensing.

Cell-free synthetic biology reactions, which are self-contained and nonbiochemical systems, offer excellent solutions.[126,127] It contains all of the biomolecular components required for efficient transcription and translation. By employing porous matrices to freeze-dry these systems into shelf-stable formats, robust distribution, storage, and usage are made possible without the need for special environmental or biocontainment requirements. Wearable technology that incorporates synthetic biology may make it possible to monitor disease states, pathogen exposure, and physiological conditions noninvasively.

Based on this principle, Nguyen et al. integrated a freeze-dried cell-free (FDCF) reaction with the CRISPR/Cas12a/Cas13a system onto a flexible textile substrate (Figure 12b).[124] This substrate can be activated through simple rehydration and enables the detection of molecular targets in respiration and the environment by using colorimetric, fluorescent, and bioluminescent techniques. The design features two layers of hydrophobic patterned fabrics interwoven with polymeric optic fibers (POFs) in a coplanar arrangement, embedding both the FDCF reaction elements and the excitation and emission illumination components. When a sample enters through the input port, it rehydrates the FDCF synthetic bioreaction immobilized within the hydrophilic textile fibers, activating the sensor circuitry. The excitation POF is illuminated by an array of LEDs, while the emission POF is bundled into a backbone and connected to the optical sensor of a wearable spectrometer, enabling the generation of fluorescent or luminescent signals for digital quantitative analysis. The method achieves a limit of detection (LOD) comparable to that of qPCR. Additionally, the technique was incorporated into a biosensor mask designed for noninvasive respiratory aerosol sampling and analysis. This portable system allows users to perform SARS-CoV-2 detection at room temperature within 90 min by simply pressing a button. However, the biosensor's reproducibility requires further improvement due to challenges posed by RNase contamination. Addressing this issue could involve incorporation of an internal RNase contamination reference to enhance reliability. Potential applications of this biosensor extend to clinicians, healthcare workers, and researchers operating in environments with specific chemical or biological threats, suspected hazards, or high-risk areas. For example, integrating the sensor into hospital white coats could trigger alarms to help prevent the spread of nosocomial infections, showcasing its potential to enhance safety and infection control in healthcare settings.

A smartphone-enabled digital CRISPR platform was developed for rapid and portable quantification of HIV RNA (Figure 12c).[125] The digitization of the RT-RPA-CRISPR/Cas12a assay facilitated quantification and accelerated the test speed, especially for low RNA concentrations. The device can detect HIV RNA within 15 min, achieving an LOD of 75 copies and a dynamic range spanning at least 2 orders of

https://doi.org/10.1021/acsnano.5c03474
ACS Nano XXXX, XXX, XXX−XXX

magnitude. Additionally, deep learning algorithms were employed to analyze fluorescence images captured by the device, offering superior accuracy in identifying positive reaction wells compared with traditional methods such as ImageJ and threshold-based analysis.

CRISPR-based wearable digital technologies enable real-time, continuous monitoring of biological processes, allowing for noninvasive or minimally invasive detection of disease-related genetic mutations or changes in gene expression. These devices could serve as convenient platforms for gene therapy, with applications in disease diagnosis, drug development, and personalized medicine.[118,119,124,128] However, CRISPR-based wearable technologies are still in their early stages. Current wearable microfluidic devices mainly focus on nucleic acid detection rather than on macromolecules. Many CRISPR-based biosensors also depend on time-consuming amplification steps, which are impractical for wearable applications. Additionally, these devices need more robust methods for precise signal output. If CRISPR-based wearable microfluidic devices can match the efficiency and reliability of tools such as the Abbott blood glucose meter, they could revolutionize the bioanalysis and diagnostics industry.

As the biofunctional potential of micronano chips continues to be explored, digital CRISPR technology demonstrates significant promise for biomedical applications. Li et al. employed a digital cell microfluidic platform to investigate the effects of zinc oxide nanorod arrays (ZnO NRs) on breast cancer cells.[129] This platform facilitates single-cell analysis of breast cancer cells following exposure to ZnO NRs and enables the simultaneous detection of 12 cytokines. Its key strengths include single-cell resolution, multiplexed cytokine detection, high-throughput capabilities, and physiological relevance. Moreover, bionanomaterial-based platforms are paving the way for the future advancement of digital CRISPR sensing in biomedical applications.[130] These platforms exhibit unique properties and capabilities, offering innovative approaches with the potential to transform the use of digital CRISPR sensing across critical domains.

7. OUTLOOK AND PERSPECTIVE

CRISPR technology plays a crucial role in promoting precise detection for multidisciplinary fields. However, issues such as overreliance on amplification, susceptibility to false positives, lack of quantification strategies, and operational complexity impede its further application. This review focuses on CRISPR digital biosensors, which address these challenges by integrating micronano collaborative chips and CRISPR technology. These biosensors can be summarized in the following five points: (1) Droplet-based CRISPR digital biosensors for quantitative determination; (2) Microarray-based CRISPR digital biosensors for semiautomated detection and reducing manpower requirements; (3) CRISPR digital biosensors with amplification strategies for highly sensitive detection; (4) CRISPR digital biosensors with amplification-free strategies to avoid false positives and simplify the detection process; (5) Applications of CRISPR digital sensing in multigene detection and wearable technology.

CRISPR digital sensing technology, utilizing droplet microfluidics, microarray chips, and wearable devices, holds great promise for various applications. Droplet microfluidics-based CRISPR biosensors enable high-throughput, sensitive nucleic acid detection. They can quickly identify specific pathogen gene sequences, making them valuable for early disease diagnosis and epidemic prevention, such as in COVID-19 detection. Microarray chip-based CRISPR biosensors allow the simultaneous analysis of multiple targets. They are widely used in genetic research and precision medicine such as detecting cancer-related gene mutations to guide targeted therapies. Wearable CRISPR biosensors enable real-time, continuous monitoring of health and fitness. They can detect disease-related gene changes noninvasively or minimally invasively, supporting early diagnosis and personalized treatment.

Droplet microfluidic chips and microarray chips are widely used in CRISPR digitization, combining both amplification and amplification-free strategies. Specialized digital CRISPR chips, such as vortex-driven, electrokinetic-driven, and membrane-driven droplets, introduce innovative approaches for CRISPR applications. Amplification-based CRISPR biosensors offer high sensitivity and rely on well-established methods, but they are labor-intensive, time-consuming, and prone to false positives. In contrast, amplification-free methods are simpler and more practical but require advanced technologies, such as high-precision micronano chips and customized CRISPR assays. Regardless of the strategy, reducing the reaction times remains a critical goal. Compared to droplet microfluidic biosensors, microarray-based CRISPR biosensors have faster initial detection speeds since they skip droplet formation. However, due to fewer reaction channels, microarray chips saturate at high concentrations, resulting in a linear detection range shorter than that of droplet microfluidics. These two approaches can complement each other, combining their strengths to achieve better detection outcomes. However, to compete as the next generation of molecular diagnostics, CRISPR digital biosensors need improvement in robustness, usability, and automation to match the advances that nucleic acid amplification has made over the last two decades. Here are their specific prospective directions:

Cas Proteins Exploration: Discovering modified Cas proteins is key to digital CRISPR technology. For example, the newly discovered Cas14 protein allows for RNA-guided single-stranded DNA targeting without a PAM sequence, simplifying CRISPR nuclease function. Research on Cas12a led to a "split-recombination" system, where crRNA divides into two modules that recombine with Cas12a to form a biologically active nucleoprotein complex, enabling instant, amplification-free RNA detection. Although the benefits of these proteins for CRISPR digital biosensor are not clear, they point to future research directions. Expect to find more highly active, precisely targeting, and uniquely cleaving proteins to enrich gene-editing tools and drive CRISPR diagnostic technology.

CRISPR-Artificial Intelligence (AI) Integration: CRISPR technology offers unparalleled precision in gene editing, while AI enhances data processing and analysis, opening new possibilities for CRISPR digital biosensors. AI can optimize guide RNA (gRNA) design, predict the gRNA-target binding efficiency, and analyze high-throughput CRISPR data. This integration improves the identification of single-nucleotide variations, reduces false positives, and enhances the assessment of gene-editing outcomes. Combining computer-controlled microfluidic chips with CRISPR further boosts automation, increases throughput, and enables precise control over reactions. Additionally, AI-powered diagnostic tools can rapidly interpret CRISPR results, enabling faster disease diagnosis and advancing personalized medicine and precision diagnostics.

https://doi.org/10.1021/acsnano.5c03474
ACS Nano XXXX, XXX, XXX−XXX

Micronano Fabrication in CRISPR Biochips: Advances in technology allow integrating all functional units on a single chip for fully automated detection, reducing errors and contamination. 3D and 4D printing offer new ways for CRISPR-based digital biochips. 3D printing enables custom biochip prototyping for specific CRISPR applications, and 4D printing adds time-dependent shape transformation, enabling dynamic digital CRISPR biochips. For example, a 4D-printed droplet microfluidic chip can keep droplets separate for easy loading, automatically merge them for reactions, and transition to subsequent steps, streamlining the process and reducing human intervention and errors. These fabrication advancements drive next-generation CRISPR biochips.

Deeper CRISPR-Based Single-cell Analysis: Digital CRISPR overcomes traditional bulk-detection limitations, enabling single-molecule characterization. In-depth single-cell analysis at the transcriptional, translational, and epigenetic levels could be further studied. When combined with microfluidics, it uncovers the impact of genetic modifications on cell function, providing precise data for cell biology research. It also helps monitor Cas proteins, enhancing gene-editing precision and single-cell analysis efficiency.

POCT and Home Testing Advances: Growing demand for POCT and home testing faces limitations as the CRISPR digital biosensor remains largely lab-bound. Expanding its use requires automated, integrated systems with higher sensitivity and portable imaging. Disposable CRISPR detection kits paired with smartphone-compatible devices could enable nonexperts to perform early disease detection, making advanced diagnostics accessible and user-friendly.

CRISPR digital biosensors, as powerful detection platforms, have the potential to lead next-generation biosensing technologies. By integrating with micronano collaborative chips, they can enhance detection performance in molecular detection and POCT, competing with digital nucleic acid amplification detection. Multidisciplinary integration of medicine, materials science, engineering, and AI will unlock their biosensing potential.

AUTHOR INFORMATION

Corresponding Authors

Xinyi Wang − *Ministry of Education Engineering Research Center of Smart Microsensors and Microsystems, School of Electronics and Information, Hangzhou Dianzi University, Hangzhou 310018, China; Key Laboratory of Micro-Nano Sensing and IoT of Wenzhou, Wenzhou Institute of Hangzhou Dianzi University, Wenzhou 325038, China;* orcid.org/0000-0001-9511-7209; Email: wxy317@hdu.edu.cn

Minghao Wang − *Ministry of Education Engineering Research Center of Smart Microsensors and Microsystems, School of Electronics and Information, Hangzhou Dianzi University, Hangzhou 310018, China; Key Laboratory of Micro-Nano Sensing and IoT of Wenzhou, Wenzhou Institute of Hangzhou Dianzi University, Wenzhou 325038, China*; Email: mhwang@hdu.edu.cn

Dujuan Li − *Ministry of Education Engineering Research Center of Smart Microsensors and Microsystems, School of Electronics and Information, Hangzhou Dianzi University, Hangzhou 310018, China*; Email: dujuanli@hdu.edu.cn

Gaofeng Wang − *Ministry of Education Engineering Research Center of Smart Microsensors and Microsystems, School of Electronics and Information, Hangzhou Dianzi University, Hangzhou 310018, China*; Email: gaofeng@hdu.edu.cn

Authors

Longjie Zhong − *Zhejiang Cancer Hospital, Hangzhou Institute of Medicine (HIM), Chinese Academy of Sciences, Hangzhou, Zhejiang 310022, China*

Wenbin Zhang − *Ministry of Education Engineering Research Center of Smart Microsensors and Microsystems, School of Electronics and Information, Hangzhou Dianzi University, Hangzhou 310018, China; Key Laboratory of Micro-Nano Sensing and IoT of Wenzhou, Wenzhou Institute of Hangzhou Dianzi University, Wenzhou 325038, China*

Pengde Wu − *Ministry of Education Engineering Research Center of Smart Microsensors and Microsystems, School of Electronics and Information, Hangzhou Dianzi University, Hangzhou 310018, China; Key Laboratory of Micro-Nano Sensing and IoT of Wenzhou, Wenzhou Institute of Hangzhou Dianzi University, Wenzhou 325038, China*

Linxi Dong − *Ministry of Education Engineering Research Center of Smart Microsensors and Microsystems, School of Electronics and Information, Hangzhou Dianzi University, Hangzhou 310018, China*

Complete contact information is available at: https://pubs.acs.org/10.1021/acsnano.5c03474

Notes

The authors declare no competing financial interest.

ACKNOWLEDGMENTS

This research was supported by Zhejiang Provincial Natural Science Foundation of China under Grant No. LQ24H180009, the Fundamental Research Funds for the Provincial Universities of Zhejiang under Grant No. GK259909299001-017, “Pioneer” and “Leading Goose” R&D Program of Zhejiang (2024C03002), and the National Natural Science Foundation of China under Grant No. 92373202.

VOCABULARY

Confinement effect: spatial restriction at micro/nanoscales that significantly alters the physical, chemical, or biological properties of materials or molecules, commonly exploited to enhance catalytic efficiency, energy storage capacity, and molecular detection sensitivity.

Trans-cleavage activity: enzymatic property of certain Cas proteins that induces nonspecific degradation of surrounding single-stranded nucleic acids after target recognition, enabling ultrasensitive molecular detection through signal amplification.

CRISPR digitization: quantifies and analyzes CRISPR-based gene editing outcomes through computational algorithms and digital signal processing.

Micronano chips: miniaturized integrated devices fabricated at micrometer to nanometer scales that combine electronic, fluidic, and optical components to perform high-precision biological/chemical analyses.

Biological detection: identifies and quantifies biological entities (cells, proteins, nucleic acids, etc.) or their interactions through physicochemical transduction mechanisms, forming the technological foundation for modern medical diagnostics, environmental monitoring, and biosecurity applications.

https://doi.org/10.1021/acsnano.5c03474
ACS Nano XXXX, XXX, XXX−XXX

REFERENCES

(1) Luo, Z.; Ang, M. J. Y.; Chan, S. Y.; Yi, Z.; Goh, Y. Y.; Yan, S.; Tao, J.; Liu, K.; Li, X.; Zhang, H.; et al. Combating the Coronavirus Pandemic: Early Detection, Medical Treatment, and a Concerted Effort by the Global Community. *Research* **2020**, *2020*, No. 6925296.

(2) Zhan, X.; Zhou, J.; Jiang, Y.; An, P.; Luo, B.; Lan, F.; Ying, B.; Wu, Y. DNA Tetrahedron-Based Crispr Bioassay for Treble-Self-Amplified and Multiplex Hpv-DNA Detection with Elemental Tagging. *Biosens. Bioelectron.* **2023**, *229*, No. 115229.

(3) Chertow, D. S. J. s. Next-Generation Diagnostics with Crispr. *Science* **2018**, *360* (6387), 381−382.

(4) Eisenstein, M. Seven Technologies to Watch in 2022. *Nature* **2022**, *601* (7894), 658−661.

(5) Barrangou, R.; Doudna, J. A. Applications of Crispr Technologies in Research and Beyond. *Nat. Biotechnol.* **2016**, *34* (9), 933−941.

(6) Li, P.; Xiong, H.; Yang, B.; Jiang, X.; Kong, J.; Fang, X. Recent Progress in Crispr-Based Microfluidic Assays and Applications. *TrAC Trends in Analytical Chemistry* **2022**, *157*, No. 116812.

(7) Makarova, K. S.; Haft, D. H.; Barrangou, R.; Brouns, S. J. J.; Charpentier, E.; Horvath, P.; Moineau, S.; Mojica, F. J. M.; Wolf, Y. I.; Yakunin, A. F.; et al. Evolution and Classification of the Crispr−Cas Systems. *Nat. Rev. Microbiol* **2011**, *9* (6), 467−477.

(8) Swarts, D. C.; Jinek, M. J. M. c. Mechanistic Insights into the Cis-and Trans-Acting Dnase Activities of Cas12a. *Mol. Cell* **2019**, *73* (3), 589−600.

(9) Gootenberg, J. S.; Abudayyeh, O. O.; Lee, J. W.; Essletzbichler, P.; Dy, A. J.; Joung, J.; Verdine, V.; Donghia, N.; Daringer, N. M.; Freije, C. A.; et al. Nucleic Acid Detection with Crispr-Cas13a/C2c2. *Science* **2017**, *356* (6336), 438−442.

(10) Zetsche, B.; Gootenberg, J. S.; Abudayyeh, O. O.; Slaymaker, I. M.; Makarova, K. S.; Essletzbichler, P.; Volz, S. E.; Joung, J.; Van Der Oost, J.; Regev, A. J. c.; et al. Cpf1 Is a Single Rna-Guided Endonuclease of a Class 2 Crispr-Cas System. *Cell* **2015**, *163* (3), 759−771.

(11) Chen, J. S.; Ma, E.; Harrington, L. B.; Da Costa, M.; Tian, X.; Palefsky, J. M.; Doudna, J. A. Crispr-Cas12a Target Binding Unleashes Indiscriminate Single-Stranded Dnase Activity. *Science* **2018**, *360* (6387), 436−439.

(12) Harrington, L. B.; Burstein, D.; Chen, J. S.; Paez-Espino, D.; Ma, E.; Witte, I. P.; Cofsky, J. C.; Kyrpides, N. C.; Banfield, J. F.; Doudna, J. A. Programmed DNA Destruction by Miniature Crispr-Cas14 Enzymes. *Science* **2018**, *362* (6416), 839−842.

(13) Makarova, K. S.; Wolf, Y. I.; Iranzo, J.; Shmakov, S. A.; Alkhnbashi, O. S.; Brouns, S. J. J.; Charpentier, E.; Cheng, D.; Haft, D. H.; Horvath, P.; et al. Evolutionary Classification of Crispr−Cas Systems: A Burst of Class 2 and Derived Variants. *Nat. Rev. Microbiol* **2020**, *18* (2), 67−83.

(14) Li, S. Y.; Cheng, Q. X.; Liu, J. K.; Nie, X. Q.; Zhao, G. P.; Wang, J. Crispr-Cas12a Has Both Cis- and Trans-Cleavage Activities on Single-Stranded DNA. *Cell Research* **2018**, *28* (4), 491−493.

(15) Sha, Y.; Huang, R.; Huang, M.; Yue, H.; Shan, Y.; Hu, J.; Xing, D. Cascade Crispr/Cas Enables Amplification-Free Microrna Sensing with Fm-Sensitivity and Single-Base-Specificity. *Chem. Commun.* **2021**, *57* (2), 247−250.

(16) Wang, J. Y.; Doudna, J. A. Crispr Technology: A Decade of Genome Editing Is Only the Beginning. *Science* **2023**, *379* (6629), No. eadd8643.

(17) Shi, K.; Xie, S.; Tian, R.; Wang, S.; Lu, Q.; Gao, D.; Lei, C.; Zhu, H.; Nie, Z. A Crispr-Cas Autocatalysis-Driven Feedback Amplification Network for Supersensitive DNA Diagnostics. *Sci. Adv.* **2021**, *7* (5), No. eabc7802.

(18) Zhao, X.; He, Y.; Shao, S.; Ci, Q.; Chen, L.; Lu, X.; Liu, Q.; Chen, J. Crispr/Cas14 and G-Quadruplex Dnazyme-Driven Biosensor for Paper-Based Colorimetric Detection of African Swine Fever Virus. *Acs Sensors* **2024**, *9* (5), 2413−2420.

(19) Yin, L.; Duan, N.; Chen, S.; Yao, Y.; Liu, J.; Ma, L. Ultrasensitive Pathogenic Bacteria Detection by a Smartphone-Read G-Quadruplex-Based Crispr-Cas12a Bioassay. *Sens. Actuators, B* **2021**, *347*, No. 130586.

(20) Ding, L.; Wu, Y.; Liu, L.-e.; He, L.; Yu, S.; Effah, C. Y.; Liu, X.; Qu, L.; Wu, Y. Universal Dnazyme Walkers-Triggered Crispr-Cas12a/Cas13a Bioassay for the Synchronous Detection of Two Exosomal Proteins and Its Application in Intelligent Diagnosis of Cancer. *Biosens. Bioelectron.* **2023**, *219*, No. 114827.

(21) Huang, Z.; Tian, D.; Liu, Y.; Lin, Z.; Lyon, C. J.; Lai, W.; Fusco, D.; Drouin, A.; Yin, X.; Hu, T.; et al. Ultra-Sensitive and High-Throughput Crispr-P Owered Covid-19 Diagnosis. *Biosens. Bioelectron.* **2020**, *164*, No. 112316.

(22) Zhang, Y.; Wu, Y.; Wu, Y.; Chang, Y.; Liu, M. Crispr-Cas Systems: From Gene Scissors to Programmable Biosensors. *TrAC Trends in Analytical Chemistry* **2021**, *137*, No. 116210.

(23) Rananaware, S. R.; Vesco, E. K.; Shoemaker, G. M.; Anekar, S. S.; Sandoval, L. S. W.; Meister, K. S.; Macaluso, N. C.; Nguyen, L. T.; Jain, P. K. Programmable Rna Detection with Crispr-Cas12a. *Nat. Commun.* **2023**, *14* (1), 5409.

(24) Joung, J.; Ladha, A.; Saito, M.; Kim, N.-G.; Woolley, A. E.; Segel, M.; Barretto, R. P. J.; Ranu, A.; Macrae, R. K.; Faure, G.; et al. Detection of Sars-Cov-2 with Sherlock One-Pot Testing. *New Engl. J. Med.* **2020**, *383* (15), 1492−1494.

(25) Ding, X.; Yin, K.; Li, Z.; Lalla, R. V.; Ballesteros, E.; Sfeir, M. M.; Liu, C. Ultrasensitive and Visual Detection of Sars-Cov-2 Using All-in-One Dual Crispr-Cas12a Assay. *Nat. Commun.* **2020**, *11* (1), 4711.

(26) Zhuang, S.; Hu, T.; Zhou, H.; He, S.; Li, J.; Zhang, Y.; Gu, D.; Xu, Y.; Chen, Y.; Wang, J. Crispr-Holmes-Based Nad+ Detection. *Front. Bioeng. Biotechnol.* **2024**, *12*, No. 1355640.

(27) Sohail, M.; Xie, S.; Zhang, X.; Li, B. Methodologies in Visualizing the Activation of Crispr/Cas: The Last Mile in Developing Crispr-Based Diagnostics and Biosensing − a Review. *Anal. Chim. Acta* **2022**, *1205*, No. 339541.

(28) Li, H.; Xiu, L.; Guo, X.; Hu, Q.; Yin, K. Spatiotemporal Dual-Dimensional Separation Enables Ultra-Simple One-Pot Crispr-Based Molecular Diagnostics. *Chem. Eng. J.* **2024**, *482*, No. 148872.

(29) Gootenberg, J. S.; Abudayyeh, O. O.; Kellner, M. J.; Joung, J.; Collins, J. J.; Zhang, F. J. S. Multiplexed and Portable Nucleic Acid Detection Platform with Cas13, Cas12a, and Csm6. *Science* **2018**, *360* (6387), 439−444.

(30) Gootenberg, J. S.; Abudayyeh, O. O.; Lee, J. W.; Essletzbichler, P.; Dy, A. J.; Joung, J.; Verdine, V.; Donghia, N.; Daringer, N. M.; Freije, C. A. J. S.; et al. Nucleic Acid Detection with Crispr-Cas13a/C2c2. *Science* **2017**, *356* (6336), 438−442.

(31) Li, H.; Xie, Y.; Chen, F.; Bai, H.; Xiu, L.; Zhou, X.; Guo, X.; Hu, Q.; Yin, K. Amplification-Free Crispr/Cas Detection Technology: Challenges, Strategies, and Perspectives. *Chem. Soc. Rev.* **2023**, *52* (1), 361−382.

(32) Li, Y.; Liu, Y.; Tang, X.; Qiao, J.; Kou, J.; Man, S.; Zhu, L.; Ma, L. Crispr/Cas-Powered Amplification-Free Detection of Nucleic Acids: Current State of the Art, Challenges, and Futuristic Perspectives. *Acs Sensors* **2023**, *8* (12), 4420−4441.

(33) Ma, L.; Zhang, W.; Yin, L.; Li, Y.; Zhuang, J.; Shen, L.; Man, S. A Sers-Signalled, Crispr/Cas-Powered Bioassay for Amplification-Free and Anti-Interference Detection of Sars-Cov-2 in Foods and Environmental Samples Using a Single Tube-in-Tube Vessel. *J. Hazard. Mater.* **2023**, *452*, No. 131195.

(34) Teng, F.; Guo, L.; Cui, T.; Wang, X.-G.; Xu, K.; Gao, Q.; Zhou, Q.; Li, W. Cdetection: Crispr-Cas12b-Based DNA Detection with Sub-Attomolar Sensitivity and Single-Base Specificity. *Genome Biol.* **2019**, *20* (1), 132.

(35) Politza, A. J.; Nouri, R.; Guan, W. Digital Crispr Systems for the Next Generation of Nucleic Acid Quantification. *TrAC Trends in Analytical Chemistry* **2023**, *159*, No. 116917.

(36) Wu, X.; Tay, J. K.; Goh, C. K.; Chan, C.; Lee, Y. H.; Springs, S. L.; Wang, D. Y.; Loh, K. S.; Lu, T. K.; Yu, H. Digital Crispr-Based Method for the Rapid Detection and Absolute Quantification of Nucleic Acids. *Biomaterials* **2021**, *274*, No. 120876.

https://doi.org/10.1021/acsnano.5c03474
ACS Nano XXXX, XXX, XXX−XXX

(37) Park, J. S.; Hsieh, K.; Chen, L.; Kaushik, A.; Trick, A. Y.; Wang, T.-H. Digital Crispr/Cas-Assisted Assay for Rapid and Sensitive Detection of Sars-Cov-2. *Adv. Sci.* **2021**, *8* (5), No. 2003564.
(38) Wang, D.; Wang, X.; Ye, F.; Zou, J.; Qu, J.; Jiang, X. An Integrated Amplification-Free Digital Crispr/Cas-Assisted Assay for Single Molecule Detection of Rna. *ACS Nano* **2023**, *17* (8), 7250−7256.
(39) Yin, W.; Zhuang, J.; Li, J.; Xia, L.; Hu, K.; Yin, J.; Mu, Y. Digital Recombinase Polymerase Amplification, Digital Loop-Mediated Isothermal Amplification, and Digital Crispr-Cas Assisted Assay: Current Status, Challenges, and Perspectives. *Small* **2023**, *19* (49), No. 2303398.
(40) Lu, L.; Zhang, H.; Lin, F.; Zhou, L.; Zhu, Z.; Yang, C. Sensitive and Automated Detection of Bacteria by Crispr/Cas12a-Assisted Amplification with Digital Microfluidics. *Sens. Actuators, B* **2023**, *381*, No. 133409.
(41) Jiang, C.; Zheng, X.; Lin, L.; Li, X.; Li, X.; Liao, Y.; Jia, W.; Shu, B. Crispr Cas12a-Mediated Amplification-Free Digital DNA Assay Improves the Diagnosis and Surveillance of Nasopharyngeal Carcinoma. *Biosens. Bioelectron.* **2023**, *237*, No. 115546.
(42) Wu, X.; Lou, X.; Zhou, H.; Raymond, J. J.; Kwang, L. G.; Ong, F. Y. T.; Springs, S. L.; Yu, H. Detection and Absolute Quantification Biosensing Tools for Food Authentication: Crispr/Cas, Digital Crispr and Beyond. *Trends in Food Science & Technology* **2024**, *145*, No. 104349.
(43) Zuo, L.; Miao, J.; He, D.; Fang, Z.; Zhang, X.; Sun, C.; Deng, X.; Ma, X.; Yu, C.; Wong, G. Development and Characterization of a Digital Crispr/Cas13a Based Assay for Rapid and Sensitive Diagnosis of Severe Fever with Thrombocytopenia Syndrome Virus. *Sens. Actuators, B* **2023**, *388*, No. 133789.
(44) Ji, Y.; Cai, G.; Liang, C.; Gao, Z.; Lin, W.; Ming, Z.; Feng, S.; Zhao, H. A Microfluidic Immunosensor Based on Magnetic Separation for Rapid Detection of Okadaic Acid in Marine Shellfish. *Anal. Chim. Acta* **2023**, *1239*, No. 340737.
(45) Safdar, S.; Ven, K.; van Lent, J.; Pavie, B.; Rutten, I.; Dillen, A.; Munck, S.; Lammertyn, J.; Spasic, D. DNA-Only, Microwell-Based Bioassay for Multiplex Nucleic Acid Detection with Single Base-Pair Resolution Using Mnazymes. *Biosens. Bioelectron.* **2020**, *152*, No. 112017.
(46) Dong, J.; Li, G.; Xia, L. Microfluidic Magnetic Spatial Confinement Strategy for the Enrichment and Ultrasensitive Detection of Mcf-7 and Escherichia Coli O157:H7. *Anal. Chem.* **2022**, *94* (48), 16901−16909.
(47) Wu, M.; Huang, Y.; Huang, Y.; Wang, H.; Li, M.; Zhou, Y.; Zhao, H.; Lan, Y.; Wu, Z.; Jia, C.; et al. Droplet Magnetic-Controlled Microfluidic Chip Integrated Nucleic Acid Extraction and Amplification for the Detection of Pathogens and Tumor Mutation Sites. *Anal. Chim. Acta* **2023**, *1271*, No. 341469.
(48) Rissin, D. M.; Kan, C. W.; Campbell, T. G.; Howes, S. C.; Fournier, D. R.; Song, L.; Piech, T.; Patel, P. P.; Chang, L.; Rivnak, A. J.; et al. Single-Molecule Enzyme-Linked Immunosorbent Assay Detects Serum Proteins at Subfemtomolar Concentrations. *Nat. Biotechnol.* **2010**, *28* (6), 595−599.
(49) Cai, G.; Yang, Z.; Chen, Y.-C.; Huang, Y.; Liang, L.; Feng, S.; Zhao, J. Magnetic Bead Manipulation in Microfluidic Chips for Biological Application. *Cyborg Bionic Syst.* **2023**, *4*, 0023.
(50) Cui, J. Q.; Liu, F. X.; Park, H.; Chan, K. W.; Leung, T.; Tang, B. Z.; Yao, S. Droplet Digital Recombinase Polymerase Amplification (Ddrpa) Reaction Unlocking Via Picoinjection. *Biosens. Bioelectron.* **2022**, *202*, No. 114019.
(51) Wu, H.; Cao, X.; Meng, Y.; Richards, D.; Wu, J.; Ye, Z.; deMello, A. J. Dropcrispr: A Lamp-Cas12a Based Digital Method for Ultrasensitive Detection of Nucleic Acid. *Biosens. Bioelectron.* **2022**, *211*, No. 114377.
(52) Luo, X.; Xue, Y.; Ju, E.; Tao, Y.; Li, M.; Zhou, L.; Yang, C.; Zhou, J.; Wang, J. Digital Crispr/Cas12b-Based Platform Enabled Absolute Quantification of Viral Rna. *Anal. Chim. Acta* **2022**, *1192*, No. 339336.
(53) Luo, X.; Wan, Y.; Wang, K.; Wei, Q.; Yu, Z.; Chen, L.; Zhou, J.; Wang, J. Digital Crispr/Cas12a-Based Platform for Precise Quantification of Telomerase Activity. *Sens. Actuators, B* **2023**, *394*, No. 134374.
(54) Nouri, R.; Jiang, Y.; Politza, A. J.; Liu, T.; Greene, W. H.; Zhu, Y.; Nunez, J. J.; Lian, X.; Guan, W. Stamp-Based Digital Crispr-Cas13a for Amplification-Free Quantification of Hiv-1 Plasma Viral Loads. *ACS Nano* **2023**, *17* (11), 10701−10712.
(55) Yue, H.; Shu, B.; Tian, T.; Xiong, E.; Huang, M.; Zhu, D.; Sun, J.; Liu, Q.; Wang, S.; Li, Y.; et al. Droplet Cas12a Assay Enables DNA Quantification from Unamplified Samples at the Single-Molecule Level. *Nano Lett.* **2021**, *21* (11), 4643−4653.
(56) Liu, F. X.; Cui, J. Q.; Park, H.; Chan, K. W.; Leung, T.; Tang, B. Z.; Yao, S. Isothermal Background-Free Nucleic Acid Quantification by a One-Pot Cas13a Assay Using Droplet Microfluidics. *Anal. Chem.* **2022**, *94* (15), 5883−5892.
(57) Tian, T.; Shu, B.; Jiang, Y.; Ye, M.; Liu, L.; Guo, Z.; Han, Z.; Wang, Z.; Zhou, X. An Ultralocalized Cas13a Assay Enables Universal and Nucleic Acid Amplification-Free Single-Molecule Rna Diagnostics. *ACS Nano* **2021**, *15* (1), 1167−1178.
(58) Xue, Y.; Luo, X.; Xu, W.; Wang, K.; Wu, M.; Chen, L.; Yang, G.; Ma, K.; Yao, M.; Zhou, Q.; et al. Pddcas: A Polydisperse Droplet Digital Crispr/Cas-Based Assay for the Rapid and Ultrasensitive Amplification-Free Detection of Viral DNA/Rna. *Anal. Chem.* **2023**, *95* (2), 966−975.
(59) Zhao, Y.; Chen, D.; Xu, Z.; Li, T.; Zhu, J.; Hu, R.; Xu, G.; Li, Y.; Yang, Y.; Liu, M. Integrating Crispr-Cas12a into a Microfluidic Dual-Droplet Device Enables Simultaneous Detection of Hpv16 and Hpv18. *Anal. Chem.* **2023**, *95* (6), 3476−3485.
(60) Ding, X.; Yin, K.; Li, Z.; Sfeir, M. M.; Liu, C. Sensitive Quantitative Detection of Sars-Cov-2 in Clinical Samples Using Digital Warm-Start Crispr Assay. *Biosens. Bioelectron.* **2021**, *184*, No. 113218.
(61) Wu, X.; Chan, C.; Springs, S. L.; Lee, Y. H.; Lu, T. K.; Yu, H. A Warm-Start Digital Crispr/Cas-Based Method for the Quantitative Detection of Nucleic Acids. *Anal. Chim. Acta* **2022**, *1196*, No. 339494.
(62) Xia, L.; Yin, J.; Zhuang, J.; Yin, W.; Zou, Z.; Mu, Y. Adsorption-Free Self-Priming Direct Digital Dual-Crrna Crispr/Cas12a-Assisted Chip for Ultrasensitive Detection of Pathogens. *Anal. Chem.* **2023**, *95* (10), 4744−4752.
(63) Zhang, C.; Cai, Z.; Zhou, Z.; Li, M.; Hong, W.; Zhou, W.; Yu, D.; Wei, P.; He, J.; Wang, Y.; et al. Casmart, a One-Step Crispr Cas12a-Mediated Isothermal Amplification for Rapid and High-Resolution Digital Detection of Rare Mutant Alleles. *Biosens. Bioelectron.* **2023**, *222*, No. 114956.
(64) Shinoda, H.; Taguchi, Y.; Nakagawa, R.; Makino, A.; Okazaki, S.; Nakano, M.; Muramoto, Y.; Takahashi, C.; Takahashi, I.; Ando, J.; et al. Amplification-Free Rna Detection with Crispr−Cas13. *Commun. Biol.* **2021**, *4* (1), 476.
(65) Shang, Y.; Xing, G.; Lin, J.; Li, Y.; Lin, Y.; Chen, S.; Lin, J. Multiplex Bacteria Detection Using One-Pot Crispr/Cas13a-Based Droplet Microfluidics. *Biosens. Bioelectron.* **2024**, *243*, No. 115771.
(66) Gu, X.; Tang, Q.; Zhu, Y.; Sun, C.; Wu, L.; Ji, H.; Wang, Q.; Wu, L.; Qin, Y. Advancements of Crispr Technology in Public Health-Related Analysis. *Biosens. Bioelectron.* **2024**, *261*, No. 116449.
(67) Gines, G.; Espada, R.; Dramé-Maigné, A.; Baccouche, A.; Larrouy, N.; Rondelez, Y. Functional Analysis of Single Enzymes Combining Programmable Molecular Circuits with Droplet-Based Microfluidics. *Nat. Nanotechnol.* **2024**, *19* (6), 800−809.
(68) Zhang, Y.; Liu, H.; Nakagawa, Y.; Nagasaka, Y.; Ding, T.; Tang, S.; Yalikun, Y.; Goda, K.; Li, M. Enhanced Crispr/Cas12a-Based Quantitative Detection of Nucleic Acids Using Double Emulsion Droplets. *Biosens. Bioelectron.* **2024**, *257*, No. 116339.
(69) Li, S.; Yin, H.; Zheng, J.; Wan, Y.; Wang, K.; Yang, C.; Zhou, J.; Zhao, M.; Yuan, X.; Wang, J. Decode: Contamination-Free Digital Crispr Platform for Point-of-Care Detection of Viral DNA/Rna. *Acs Sensors* **2024**, *9* (8), 4256−4264.

https://doi.org/10.1021/acsnano.5c03474
ACS Nano XXXX, XXX, XXX−XXX

(70) Shang, L.; Cheng, Y.; Zhao, Y. Emerging Droplet Microfluidics. *Chem. Rev.* **2017**, *117* (12), 7964−8040.
(71) Kaminski, T. S.; Garstecki, P. Controlled Droplet Microfluidic Systems for Multistep Chemical and Biological Assays. *Chem. Soc. Rev.* **2017**, *46* (20), 6210−6226.
(72) Joensson, H. N.; Andersson Svahn, H. Droplet Microfluidics—a Tool for Single-Cell Analysis. *Angew. Chem., Int. Ed.* **2012**, *51* (49), 12176−12192.
(73) Sun, A. C.; Steyer, D. J.; Allen, A. R.; Payne, E. M.; Kennedy, R. T.; Stephenson, C. R. J. A Droplet Microfluidic Platform for High-Throughput Photochemical Reaction Discovery. *Nat. Commun.* **2020**, *11* (1), 6202.
(74) Jiang, Z.; Shi, H.; Tang, X.; Qin, J. Recent Advances in Droplet Microfluidics for Single-Cell Analysis. *TrAC Trends in Analytical Chemistry* **2023**, *159*, No. 116932.
(75) Hu, K.; Yu, F.; Ho, T. Y.; Chakrabarty, K. Testing of Flow-Based Microfluidic Biochips: Fault Modeling, Test Generation, and Experimental Demonstration. *IEEE Trans. Comput.-Aided Design Integr. Circuits Syst.* **2014**, *33* (10), 1463−1475.
(76) De Jonghe, J.; Kaminski, T. S.; Morse, D. B.; Tabaka, M.; Ellermann, A. L.; Kohler, T. N.; Amadei, G.; Handford, C. E.; Findlay, G. M.; Zernicka-Goetz, M.; et al. Spindrop: A Droplet Microfluidic Platform to Maximise Single-Cell Sequencing Information Content. *Nat. Commun.* **2023**, *14* (1), 4788.
(77) Postek, W.; Garstecki, P. Droplet Microfluidics for High-Throughput Analysis of Antibiotic Susceptibility in Bacterial Cells and Populations. *Acc. Chem. Res.* **2022**, *55* (5), 605−615.
(78) Yue, X.; Fang, X.; Sun, T.; Yi, J.; Kuang, X.; Guo, Q.; Wang, Y.; Gu, H.; Xu, H. Breaking through the Poisson Distribution: A Compact High-Efficiency Droplet Microfluidic System for Single-Bead Encapsulation and Digital Immunoassay Detection. *Biosens. Bioelectron.* **2022**, *211*, No. 114384.
(79) Su, F.; Chakrabarty, K.; Fair, R. B. Microfluidics-Based Biochips: Technology Issues, Implementation Platforms, and Design-Automation Challenges. *IEEE Transactions on Computer-Aided Design of Integrated Circuits and Systems* **2006**, *25* (2), 211−223.
(80) Ackerman, C. M.; Myhrvold, C.; Thakku, S. G.; Freije, C. A.; Metsky, H. C.; Yang, D. K.; Ye, S. H.; Boehm, C. K.; Kosoko-Thoroddsen, T.-S. F.; Kehe, J.; et al. Massively Multiplexed Nucleic Acid Detection with Cas13. *Nature* **2020**, *582* (7811), 277−282.
(81) Welch, N. L.; Zhu, M.; Hua, C.; Weller, J.; Mirhashemi, M. E.; Nguyen, T. G.; Mantena, S.; Bauer, M. R.; Shaw, B. M.; Ackerman, C. M.; et al. Multiplexed Crispr-Based Microfluidic Platform for Clinical Testing of Respiratory Viruses and Identification of Sars-Cov-2 Variants. *Nature Medicine* **2022**, *28* (5), 1083−1094.
(82) Xia, L.; Zhuang, J.; Zou, Z.; Yin, J.; Mu, Y. Direct Digital Polymerase Chain Reaction Chip for the Detection of Egfr T790m Mutation in Plasma. *Talanta* **2022**, *237*, No. 122977.
(83) Li, X.; Wang, T.; Liu, X.; Jiang, H.; Wang, X. Advances of Engineered Microfluidic Biosensors Via Crispr/Cas in Bacteria and Virus Monitoring. *Chem. Eng. J.* **2024**, *491*, No. 152038.
(84) Avaro, A. S.; Santiago, J. G. A Critical Review of Microfluidic Systems for Crispr Assays. *Lab Chip* **2023**, *23* (5), 938−963.
(85) Shen, J.; Chen, Z.; Xie, R.; Li, J.; Liu, C.; He, Y.; Ma, X.; Yang, H.; Xie, Z. Crispr/Cas12a-Assisted Isothermal Amplification for Rapid and Specific Diagnosis of Respiratory Virus on an Microfluidic Platform. *Biosens. Bioelectron.* **2023**, *237*, No. 115523.
(86) Li, S.-Y.; Cheng, Q.-X.; Wang, J.-M.; Li, X.-Y.; Zhang, Z.-L.; Gao, S.; Cao, R.-B.; Zhao, G.-P.; Wang, J. Crispr-Cas12a-Assisted Nucleic Acid Detection. *Cell Discovery* **2018**, *4* (1), 20.
(87) Li, L.; Li, S.; Wu, N.; Wu, J.; Wang, G.; Zhao, G.; Wang, J. Holmesv2: A Crispr-Cas12b-Assisted Platform for Nucleic Acid Detection and DNA Methylation Quantitation. *ACS Synth. Biol.* **2019**, *8* (10), 2228−2237.
(88) Notomi, T.; Okayama, H.; Masubuchi, H.; Yonekawa, T.; Watanabe, K.; Amino, N.; Hase, T. Loop-Mediated Isothermal Amplification of DNA. *Nucleic Acids Res.* **2000**, *28* (12), e63.
(89) Piepenburg, O.; Williams, C. H.; Stemple, D. L.; Armes, N. A. DNA Detection Using Recombination Proteins. *PLOS Biology* **2006**, *4* (7), No. e204.
(90) You, D.; Xu, T.; Huang, B. Z.; Wu, F.; Deng, L. S.; Liu, Z. Y.; Ge, L. P.; Liu, Z. H.; Sun, J.; Zeng, X.; et al. Rapid, Sensitive, and Visual Detection of Pseudorabies Virus with an Rpa-Crispr/Escas13d-Based Dual-Readout Portable Platform. *Anal. Chim. Acta* **2024**, *1318*, No. 342918.
(91) Yang, L.; Chen, G.; Wu, J.; Wei, W.; Peng, C.; Ding, L.; Chen, X.; Xu, X.; Wang, X.; Xu, J. A Pam-Free One-Step Asymmetric Rpa and Crispr/Cas12b Combined Assay (Oar-Crispr) for Rapid and Ultrasensitive DNA Detection. *Anal. Chem.* **2024**, *96* (14), 5471−5477.
(92) Rolando, J. C.; Jue, E.; Schoepp, N. G.; Ismagilov, R. F. Real-Time, Digital Lamp with Commercial Microfluidic Chips Reveals the Interplay of Efficiency, Speed, and Background Amplification as a Function of Reaction Temperature and Time. *Anal. Chem.* **2019**, *91* (1), 1034−1042.
(93) Lin, X.; Huang, X.; Urmann, K.; Xie, X.; Hoffmann, M. R. Digital Loop-Mediated Isothermal Amplification on a Commercial Membrane. *Acs Sensors* **2019**, *4* (1), 242−249.
(94) Zhao, Z.; Wang, R.; Yang, X.; Jia, J.; Zhang, Q.; Ye, S.; Man, S.; Ma, L. Machine Learning-Assisted, Dual-Channel Crispr/Cas12a Biosensor-in-Microdroplet for Amplification-Free Nucleic Acid Detection for Food Authenticity Testing. *ACS Nano* **2024**, *18* (49), 33505−33519.
(95) Zhao, J.; Kong, D.; Zhang, G.; Zhang, S.; Wu, Y.; Dai, C.; Chen, Y.; Yang, Y.; Liu, Y.; Wei, D. An Efficient Crispr/Cas Cooperative Shearing Platform for Clinical Diagnostics Applications. *Angew. Chem., Int. Ed.* **2024**, *63* (52), No. e202411705.
(96) Yang, Y.; Gong, F.; Shan, X.; Tan, Z.; Zhou, F.; Ji, X.; Xiang, M.; Wang, F.; He, Z. Amplification-Free Detection of Mpox Virus DNA Using Cas12a and Multiple Crrnas. *Microchim. Acta* **2024**, *191* (2), 102.
(97) Li, M.; Cai, Z.; Song, S.; Yue, X.; Lu, W.; Rao, S.; Zhang, C.; Xue, C. Eccas6e-Based Antisense Crrna for Gene Repression and Rna Editing in Microorganisms. *Nucleic Acids Res.* **2024**, *52*, No. 8628.
(98) Huang, D.; Xu, C.; Jiang, C.; Chen, Q.; Xu, Z.; Fang, X. Advances and Challenges of Signal Readout Systems in Crispr-Based Biosensors for Point-of-Care Testing of Nucleic Acid. *TrAC Trends in Analytical Chemistry* **2024**, *178*, No. 117856.
(99) Li, T.; Cheng, N. Sensitive and Portable Signal Readout Strategies Boost Point-of-Care Crispr/Cas12a Biosensors. *Acs Sensors* **2023**, *8* (11), 3988−4007.
(100) Huang, T.; Li, L.; Li, J.; Li, X.; Li, S.; Wang, X.; Zhang, N.; Yu, Y.; Zhang, X.; Zhao, Z.; et al. Rapid, Sensitive, and Visual Detection of Clonorchis Sinensis with an Rpa-Crispr/Cas12a-Based Dual Readout Portable Platform. *Int. J. Biol. Macromol.* **2023**, *249*, No. 125967.
(101) Bao, Q.; Sun, J.; Fu, X.; Sheng, L.; Ye, Y.; Ji, J.; Zhang, Y.; Wang, J.; Ping, J.; Sun, X. A Simplified Amplification-Free Strategy with Lyophilized Crispr-Ccrrna System for Drug-Resistant Salmonella Detection. *Small* **2023**, *19* (29), No. 2207343.
(102) Weng, Z.; You, Z.; Yang, J.; Mohammad, N.; Lin, M.; Wei, Q.; Gao, X.; Zhang, Y. Crispr-Cas Biochemistry and Crispr-Based Molecular Diagnostics. *Angew. Chem., Int. Ed.* **2023**, *62* (17), No. e202214987.
(103) Hu, T.; Ke, X.; Li, W.; Lin, Y.; Liang, A.; Ou, Y.; Chen, C. Crispr/Cas12a-Enabled Multiplex Biosensing Strategy Via an Affordable and Visual Nylon Membrane Readout. *Adv. Sci.* **2023**, *10* (2), No. 2204689.
(104) Sun, Y.; Huang, Y.; Qi, T.; Jin, Q.; Jia, C.; Zhao, J.; Feng, S.; Liang, L. Wet-Etched Microchamber Array Digital Pcr Chip for Sars-Cov-2 Virus and Ultra-Early Stage Lung Cancer Quantitative Detection. *ACS Omega* **2022**, *7* (2), 1819−1826.
(105) Cui, X.; Wu, L.; Wu, Y.; Zhang, J.; Zhao, Q.; Jing, F.; Yi, L.; Li, G. Fast and Robust Sample Self-Digitization for Digital Pcr. *Anal. Chim. Acta* **2020**, *1107*, 127−134.
(106) Mao, Z.; Lei, H.; Chen, R.; Ren, S.; Liu, B.; Gao, Z. Crispr Molecular Detection Techniques: Advances from Single to Multiple

https://doi.org/10.1021/acsnano.5c03474
ACS Nano XXXX, XXX, XXX−XXX

Detection Methods. *TrAC Trends in Analytical Chemistry* **2023**, *166*, No. 117198.
(107) Dong, J.; Wu, X.; Hu, Q.; Sun, C.; Li, J.; Song, P.; Su, Y.; Zhou, L. An Immobilization-Free Electrochemical Biosensor Based on Crispr/Cas13a and Fam-Rna-Mb for Simultaneous Detection of Multiple Pathogens. *Biosens. Bioelectron.* **2023**, *241*, No. 115673.
(108) Zhu, Y.; Zheng, X.; Zhu, R.; Zhao, H.; Zhai, H.; Qian, F.; Zhang, T.; Xie, Z.; Liu, S.; Jiang, B.; et al. Crispr-Cas12a Powered Multifunctional DNA Nanodumbbell Lock Biosensor for Multiple Molecular Detection. *Chem. Eng. J.* **2023**, *468*, No. 143494.
(109) Wang, H.; Li, Y. L.; Fan, Y. J.; Dong, J. X.; Ren, X.; Ma, H.; Wu, D.; Gao, Z. F.; Wei, Q.; Xia, F. DNA Tile and Invading Stacking Primer-Assisted Crispr−Cas12a Multiple Amplification System for Entropy-Driven Electrochemical Detection of Microrna with Tunable Sensitivity. *Anal. Chem.* **2023**, *95* (36), 13659−13667.
(110) Zhao, Y.; Wu, W.; Tang, X.; Zhang, Q.; Mao, J.; Yu, L.; Li, P.; Zhang, Z. A Universal Crispr/Cas12a-Powered Intelligent Point-of-Care Testing Platform for Multiple Small Molecules in the Healthcare, Environment, and Food. *Biosens. Bioelectron.* **2023**, *225*, No. 115102.
(111) Fu, J.; Zhang, L.; Long, Y.; Liu, Z.; Meng, G.; Zhao, H.; Su, X.; Shi, S. Multiplexed Crispr-Based Nucleic Acid Detection Using a Single Cas Protein. *Anal. Chem.* **2023**, *95* (44), 16089−16097.
(112) Wu, X.; Zhao, Y.; Guo, C.; Liu, C.; Zhang, Q.; Chen, Y.; Liu, Y.; Zhang, X. Ratiocrispr: A Ratiometric Biochip Based on Crispr/Cas12a for Automated and Multiplexed Detection of Heteroplasmic Snps in Mitochondrial DNA. *Biosens. Bioelectron.* **2023**, *241*, No. 115676.
(113) Gootenberg, J. S.; Abudayyeh, O. O.; Kellner, M. J.; Joung, J.; Collins, J. J.; Zhang, F. Multiplexed and Portable Nucleic Acid Detection Platform with Cas13, Cas12a, and Csm6. *Science* **2018**, *360* (6387), 439−444.
(114) Ding, L.; Wang, X.; Chen, X.; Xu, X.; Wei, W.; Yang, L.; Ji, Y.; Wu, J.; Xu, J.; Peng, C. Development of a Novel Cas13a/Cas12a-Mediated 'One-Pot' Dual Detection Assay for Genetically Modified Crops. *J. Adv. Res.* **2025**, *72*, 97.
(115) Aguirre-Ghiso, J. A. Models, Mechanisms and Clinical Evidence for Cancer Dormancy. *Nature Reviews Cancer* **2007**, *7* (11), 834−846.
(116) Li, T.; Hu, R.; Xia, J.; Xu, Z.; Chen, D.; Xi, J.; Liu, B.; Zhu, J.; Li, Y.; Yang, Y.; et al. G-Triplex: A New Type of Crispr-Cas12a Reporter Enabling Highly Sensitive Nucleic Acid Detection. *Biosens. Bioelectron.* **2021**, *187*, No. 113292.
(117) Petrosky, E.; Bocchini, J. A., Jr; Hariri, S.; Chesson, H.; Curtis, C. R.; Saraiya, M.; Unger, E. R.; Markowitz, L. E. Use of 9-Valent Human Papillomavirus (Hpv) Vaccine: Updated Hpv Vaccination Recommendations of the Advisory Committee on Immunization Practices. *MMWR Morb. Mortal Wkly. Rep.* **2015**, *64* (11), 300−304.
(118) Shi, R.; Zhong, L.; Liu, G.; Mak, W. C. Crispr/Cas Biosensing Technology: From Lab Assays to Integrated Portable Devices Towards Wearables. *TrAC Trends in Analytical Chemistry* **2024**, *177*, No. 117796.
(119) Ye, C.; Lukas, H.; Wang, M.; Lee, Y.; Gao, W. Nucleic Acid-Based Wearable and Implantable Electrochemical Sensors. *Chem. Soc. Rev.* **2024**, *53* (15), 7960−7982.
(120) Heikenfeld, J.; Jajack, A.; Feldman, B.; Granger, S. W.; Gaitonde, S.; Begtrup, G.; Katchman, B. A. Accessing Analytes in Biofluids for Peripheral Biochemical Monitoring. *Nat. Biotechnol.* **2019**, *37* (4), 407−419.
(121) Yang, Q.; Rosati, G.; Abarintos, V.; Aroca, M. A.; Osma, J. F.; Merkoçi, A. Wearable and Fully Printed Microfluidic Nanosensor for Sweat Rate, Conductivity, and Copper Detection with Healthcare Applications. *Biosens. Bioelectron.* **2022**, *202*, No. 114005.
(122) Shajari, S.; Salahandish, R.; Zare, A.; Hassani, M.; Moossavi, S.; Munro, E.; Rashid, R.; Rosenegger, D.; Bains, J. S.; Sanati Nezhad, A. Microsweat: A Wearable Microfluidic Patch for Noninvasive and Reliable Sweat Collection Enables Human Stress Monitoring. *Adv. Sci.* **2023**, *10* (7), No. 2204171.
(123) Yang, B.; Kong, J.; Fang, X. Programmable Crispr-Cas9Microneedle Patch for Long-Term Capture and Real-Time Monitoring of Universal Cell-Free DNA. *Nat. Commun.* **2022**, *13* (1), 3999.
(124) Nguyen, P. Q.; Soenksen, L. R.; Donghia, N. M.; Angenent-Mari, N. M.; de Puig, H.; Huang, A.; Lee, R.; Slomovic, S.; Galbersanini, T.; Lansberry, G.; et al. Wearable Materials with Embedded Synthetic Biology Sensors for Biomolecule Detection. *Nat. Biotechnol.* **2021**, *39* (11), 1366−1374.
(125) Ngo, H. T.; Akarapipad, P.; Lee, P.-W.; Park, J. S.; Chen, F.-E.; Trick, A. Y.; Wang, T.-H.; Hsieh, K. Rapid and Portable Quantification of Hiv Rna Via a Smartphone-Enabled Digital Crispr Device and Deep Learning. *Sensors and Actuators Reports* **2024**, *8*, No. 100212.
(126) Wang, B.; Zhao, J.; Zhang, J.; Wei, T.; Han, K.; Gao, T. Electrochemical Biosensing Interfaced with Cell-Free Synthetic Biology. *TrAC Trends in Analytical Chemistry* **2024**, *176*, No. 117756.
(127) Baranwal, A. K.; Maerkl, S. J. J. A Comprehensive Review of Microfluidic Approaches in Cell-Free Synthetic Biology. *Front. Synth. Biol.* **2024**, *2*, No. 1397533.
(128) Fellmann, C.; Gowen, B. G.; Lin, P.-C.; Doudna, J. A.; Corn, J. E. Cornerstones of Crispr−Cas in Drug Discovery and Therapy. *Nat. Rev. Drug Discovery* **2017**, *16* (2), 89−100.
(129) Li, P.; Wang, C.; Qiu, J.; Song, F.; Huang, Y.; Zhang, Y.; Zhang, K.; Ji, H.; Sang, Y.; Blaker, J. J.; et al. Inhibitory Effect of Zinc Oxide Nanorod Arrays on Breast Cancer Cells Profiled through Real-Time Cytokines Screening by a Single-Cell Microfluidic Platform. *BMEMat* **2023**, *1* (3), No. e12040.
(130) Kumar, J.; Varela-Ramirez, A.; Narayan, M. Development of Novel Carbon-Based Biomedical Platforms for Intervention in Xenotoxicant-Induced Parkinson's Disease Onset. *BMEMat* **2024**, *2* (4), No. e12072.

https://doi.org/10.1021/acsnano.5c03474
ACS Nano XXXX, XXX, XXX−XXX